

Transient High Salt Intake Promotes T-Cell-Mediated Hypertensive Vascular Injury

Peer-reviewed author version

Yakoub, Mina; Rahman, Masudur; Kleimann, Patricia; Hoffe, Jasmina; Feige, Milena; Bouvain, Pascal; Alter, Christina; Kluczny, Jennifer Isabel; Reidel, Sophia; Nederlof, Rianne; Hering, Lydia; Argov, Doron; Arifaj, Denada; Kantauskaite, Marta; Meister, Jaroslawnna; KLEINWIETFELD, Markus; Rump, Lars Christian; Jantsch, Jonathan; Floegel, Ulrich; Mueller, Dominik N.; Temme, Sebastian & Stegbauer, Johannes (2024) Transient High Salt Intake Promotes T-Cell-Mediated Hypertensive Vascular Injury. In: Hypertension, 81 (12) , p. 2415 -2429.

DOI: 10.1161/HYPERTENSIONAHA.124.23115

Handle: <http://hdl.handle.net/1942/44855>

1 **Transient high salt intake promotes T cell-mediated hypertensive vascular injury**

2 **Short Title: High salt aggravates hypertensive vascular injury**

3

4 Mina Yakoub¹, Masudur Rahman¹, Patricia Kleimann^{2,3}, Jasmina Hoffe¹, Milena Feige¹,
5 Pascal Bouvain^{2,3}, Christina Alter³, Jennifer-Isabel Kluczny¹⁶, Sophia Reidel⁴, Rianne
6 Nederlof⁴, Lydia Hering¹, Doron Argov¹, Denada Arifaj¹, Marta Kantauskaite¹, Jaroslawn
7 Meister^{5,6}, Markus Kleinewietfeld^{7,8,9}, Lars Christian Rump^{1,10}, Jonathan Jantsch¹¹, Ulrich
8 Flögel^{2,10}, Dominik N. Müller^{12,13,14,15}, Sebastian Temme^{2,10,16*}, Johannes Stegbauer^{1,10#*}

9

10 ¹ Department of Nephrology, Faculty of Medicine, University Hospital, Heinrich-Heine-
11 University, Düsseldorf, Germany

12 ² Experimental Cardiovascular Imaging, Department of Molecular Cardiology, Heinrich-
13 Heine-University, Düsseldorf, Germany

14 ³ Department of Molecular Cardiology, Heinrich-Heine-University, Düsseldorf, Germany

15 ⁴ Institut für Herz-Kreislauf-Physiologie, Heinrich-Heine-University, Düsseldorf, Germany

16 ⁵ Institute for Clinical Diabetology, German Diabetes Center, Leibniz Institute for Diabetes
17 Research at Heinrich Heine University, Düsseldorf, Germany

18 ⁶ German Center for Diabetes Research (DZD e.V.), München-Neuherberg, Germany

19 ⁷ VIB Laboratory of Translational Immunomodulation, VIB Center for Inflammation
20 Research (IRC), Hasselt University, Diepenbeek, Belgium

21 ⁸ Department of Immunology, Biomedical Research Institute, Hasselt University,
22 Diepenbeek, Belgium

23 ⁹ University Multiple Sclerosis Center (UMSC), Hasselt University, Diepenbeek, Belgium

24 ¹⁰ Cardiovascular Research Institute Düsseldorf (CARID), Medical Faculty and University
25 Hospital Düsseldorf, Heinrich-Heine-University, Düsseldorf, Germany

1 ¹¹ Institute for Medical Microbiology, Immunology and Hygiene, Center for Molecular
2 Medicine Cologne (CMMC), University of Cologne, Cologne, Germany

3 ¹² Max Delbrück Center for Molecular Medicine in the Helmholtz Association, Berlin,
4 Germany

5 ¹³ Experimental and Clinical Research Center, a cooperation of Charité-Universitätsmedizin
6 Berlin and Max Delbrück Center for Molecular Medicine, Berlin, Germany

7 ¹⁴ Charité-Universitätsmedizin Berlin, corporate member of Freie Universität Berlin and
8 Humboldt-Universität zu Berlin, Berlin, Germany

9 ¹⁵ DZHK (German Centre for Cardiovascular Research), partner site Berlin, Germany;

10 ¹⁶ Department of Anaesthesiology, Faculty of Medicine, University Hospital, Heinrich-Heine-
11 University, Düsseldorf, Germany

12 * **Equal contribution**

13

14 # **Correspondence to:**

15 Prof. Dr. med. Johannes Stegbauer

16 Department of Nephrology,

17 Faculty of Medicine, University Hospital

18 Heinrich-Heine-University, Düsseldorf

19 Universitätsstraße 1

20 40225 Düsseldorf, Germany

21 E-Mail: johannes.stegbauer@med.uni-duesseldorf.de

22 Word count: 8986

23 Figures: 5

24

1 **Abstract**

2 **Background:** Dietary high salt intake has a strong impact on cardiovascular diseases. Here
3 we investigated the link between high salt (HS)-aggravated immune responses and the
4 development of hypertensive vascular disease.

5 **Methods:** ApolipoproteinE-deficient mice were transiently treated with HS (1% NaCl) via
6 drinking water for two weeks, followed by a wash-out period, and subsequent angiotensin II
7 infusion (1000ng/kg/min for 10 days) to induce abdominal aortic aneurysms/dissections and
8 inflammation.

9 **Results:** While transient HS intake alone triggered non-pathologic infiltration of activated T
10 cells into the aorta, subsequent angiotensin II (AngII) infusion increased mortality and the
11 incidence of abdominal aortic aneurysms/dissections and atherosclerosis compared to
12 hypertensive control mice. There were no differences in blood pressure between both groups.
13 In transient HS-treated hypertensive mice, aortic injury was associated with increased
14 inflammation, accumulation of neutrophils, monocytes, CD69⁺CD4⁺ T cells, as well as CD4⁺
15 and CD8⁺ memory T cells. Mechanistically, transient HS intake increased expression levels
16 of aortic *ROR γ t* as well as splenic CD4⁺T_H17 and CD8⁺T_C1 T cells in AngII-treated mice.
17 Isolated aortas of untreated mice were incubated with supernatants of T_H17, T_H1 or T_C1 cells
18 polarized *in vitro* under HS or normal conditions which revealed that secreted factors of HS-
19 differentiated T_H17 and T_C1 cells, but not T_H1 cells accelerated endothelial dysfunction.

20 **Conclusions:** Our data suggest that transient HS intake induces a subclinical T cell-mediated
21 aortic immune response, which is enhanced by AngII. We propose a two-hit model, in which
22 HS acts as a predisposing factor to enhance hypertension-induced T_H17 and T_C1 polarization
23 and aortic disease.

24

- 1 **Keywords:** Salt, vascular inflammation, vascular injury, hypertension, effector memory cells,
- 2 CD8 T cells, Th17 cells, aortic aneurysm,
- 3

1 **Nonstandard Abbreviations and Acronyms**

2	AAA	Abdominal aortic aneurysm
3	AAD	Abdominal aortic dissection
4	AngII	AngiotensinII
5	ANOVA	Analysis of variance
6	ApoE	ApolipoproteinE
7	ApoE ^{-/-}	ApolipoproteinE deficient mice
8	A.U.	Arbitrary unit
9	BP	Blood pressure
10	CD	Cluster of differentiation
11	CVD	Cardiovascular Disease
12	EAE	Experimental autoimmune encephalomyelitis
13	FACS	Fluorescence activated cell sorting
14	FCS	Fetal calf serum
15	FMO	Fluorescence minus one
16	fMLP	N-Formylmethionyl-leucyl-phenylalanine
17	GAPDH	Glyceraldehyde-3-phosphate dehydrogenase
18	HBSS	Hank's balanced salt solution
19	HS	High Salt
20	ICAM-1	Intercellular adhesion molecule 1
21	IL	Interleukin
22	IL6	Interleukin 6

1	IL10	Interleukin 10
2	IL17	Interleukin 17
3	INF γ	Interferon γ
4	iNOS	Inducible nitric oxide synthase
5	M1	Proinflammatory macrophage
6	M2	Anti-inflammatory macrophage
7	Mgl2	Macrophage Gal/GalNAc lectin 2
8	MRI	Magnetic resonance imaging
9	mRNA	Messenger ribonucleic acid
10	NET	Neutrophil extracellular traps
11	PFC	Perfluorocarbon nanoemulsion
12	PlGF	Placental growth factor
13	PMA	Phorbol-12-myristat-13-acetat
14	qPCR	Quantitative polymerase chain reaction
15	ROR γ t	RAR-related orphan receptor γ t
16	RPMI	Roswell Park Memorial Institute
17	SEM	Standard error of mean
18	SGK1	Serum and glucocorticoid-regulated kinase 1
19	Tbx21	T-box transcription factor 21
20	T _C	Cytotoxic CD8 ⁺ T cell
21	T _{CM}	Central memory T cell
22	T _{EM}	Effector memory T cell
23	TGF β	Tumor growth factor β

- 1 T_H $CD4^+$ T helper cell
- 2 $TNF\alpha$ Tumor necrosis factor α
- 3 T_N Naïve T cells
- 4 T_{reg} Regulatory T cell
- 5

1 **1. Introduction**

2 High dietary sodium intake is a hallmark of the Western diet. According to the World Health
3 Organization, the daily salt consumption is approximately 9-12 g/day, which is about 20-fold
4 higher compared to historical intake¹. Epidemiologic and experimental data have provided
5 compelling evidence that high salt (HS) is an important factor in the development and
6 progression of cardiovascular disease (CVD)². Consequently, national, and international
7 health organizations recommend a daily salt intake of <5 g/day. One of the main reasons is
8 that high sodium intake is associated with elevated BP leading to the development or
9 progression of CVD². In addition, excessive sodium intake also has deleterious effects on
10 CVD progression through BP-independent mechanisms. High sodium intake modulates the
11 immune response leading to increased inflammation, oxidative stress, fibrosis, and finally
12 cardiovascular and renal organ dysfunction³.

13 More recently, several studies have unraveled some of the mechanisms of how HS intake
14 affects immune cell function, such as enhancing the proinflammatory activity of T cells,
15 monocytes, and macrophages^{4,5}. The underlying mechanisms are multifactorial and complex.
16 For instance, HS leads to alterations in the gut microbiome that drive the expansion of T_H17
17 cells⁶. Furthermore, hypertonic HS also induces direct T cell differentiation into effector and
18 memory T cells, especially into the T_H17⁷ and T_H1⁸ lineage, and reduces the regulatory
19 capacity of T_{regs}⁹. Hypertonic HS also promotes the differentiation of macrophages into a
20 proinflammatory M1-like phenotype by increasing osmoprotective signaling and by affecting
21 mitochondrial function¹⁰⁻¹².

22 Atherosclerosis and the formation of abdominal aortic aneurysms (AAA) are promoted by
23 elevated BP but also inflammatory processes^{13,14}. Epidemiological data indicate a link
24 between HS intake and the development of aortic diseases like AAA¹⁵ or atherosclerosis¹⁶.

1 However, the precise mechanisms of how HS intake aggravates aortic diseases are still
2 unclear. In the present study, we investigated whether the immunological impact of HS
3 aggravates Angiotensin II (AngII)-mediated aortic inflammation, leading to AAA or
4 abdominal aortic dissection (AAD). AngII-infused apolipoproteinE deficient mice (ApoE^{-/-})
5 were chosen for this study, because these mice reflect the high-risk profile of patients with
6 hypercholesterolemia and hypertension, which are prone to developing atherosclerosis, aortic
7 aneurysms, and dissections. To this end, we treated the mice transiently with HS via drinking
8 water, followed by a wash-out period with normal water for one week before implantation of
9 AngII-releasing minipumps. This protocol separates the direct effect of salt on BP elevation
10 and the priming of the immune system. We found that transient HS intake followed by AngII
11 infusion strongly promoted aortic inflammation and AAA/AAD formation but did not alter
12 BP compared to the control group only infused with AngII. Mechanistically, transient salt
13 intake induced a subclinical aortic immune response with elevated CD4⁺ T cell activation and
14 memory formation. During AngII infusion, these pre-activated CD4⁺ T cells differentiated
15 into a T_H17 and effector memory phenotype causing proinflammatory cytokines secretion,
16 endothelial dysfunction as well as increased infiltration of neutrophils, monocytes,
17 macrophages, and CD8⁺ T_C1 cells that finally resulted in aggravated hypertensive vascular
18 injury.

19

20

1 **2. Materials and Methods**

2 The authors declare that all supporting data and analytical methods are available within the
3 article and its online-only Data Supplement. The data, analytical methods, and study
4 materials that support the findings of this study are available from the corresponding author
5 upon reasonable request.

6

7 **2.1 Animal Ethics**

8 ApoE^{-/-} mice were backcrossed on a C57BL/6 background for at least 10 generations.
9 Experiments were approved by the responsible federal state authority (Landesamt für Natur-,
10 Umwelt-, und Verbraucherschutz Nordrhein-Westfalen, G301/18) and performed following
11 the guidelines from the Directive 2010/63/EU of the European Parliament on the protection
12 of animals used for scientific purposes. Mice were bred and maintained at the animal facility
13 of the University of Düsseldorf. Mice were kept on a 12:12 hour day/night cycle with
14 constant access to food and water. More details concerning the experimental animals are
15 mentioned in the supplemental table (Table S1) according to ARRIVE 2.0 guidelines.

16

17 **2.2 Statistical analysis**

18 Statistical analyses were performed with Prism (GraphPad Software). Outliers were identified
19 by Grubbs' test and excluded from the analysis. To evaluate if data points represent a
20 Gaussian distribution we used Shapiro-Wilk or Kolmogorov-Smirnov test. To compare two
21 groups, a one- or two-tailed unpaired t-test (with or without Welch's correction) or a Mann-
22 Whitney test was used if the data points did not fit a Gaussian distribution. Two-tailed tests
23 were conducted to investigate the hypothesis whether transient HS intake affects hypertensive

1 vascular injury and inflammation. One-tailed tests were conducted to test the hypothesis
2 whether transient HS intake aggravates vascular injury or immune responses. A 2-way
3 ANOVA test followed by Sidak's multiple comparison was used to compare two independent
4 variables between two groups. Survival of the mice was visualized by Kaplan-Meier curves
5 and statistically compared by using a log-rank test. A *P* value <0.05 (*) was considered
6 statistically significant. Depicted data are presented as mean ± SEM.

7

1 **3. Results**

2 **3.1 Transient high salt intake aggravates AngII-induced aortic disease**

3 To evaluate the effect of transient HS intake on vascular injury, 8–10-week-old male ApoE^{-/-}
4 mice were transiently treated with 1% salt in the drinking water or tap water (as a control for
5 normal salt) for two weeks. Afterwards, mice were returned to normal tap water for one week
6 and then osmotic minipumps filled with AngII were subcutaneously implanted for 10 days
7 (Fig. 1A). Chronic AngII infusion resulted in significantly higher mortality in transiently HS-
8 treated mice compared to control mice (33% vs. 16% at day 10, $p < 0.05$; Fig. 1B, left). Most
9 animals died from aortic rupture. Next, we investigated whether increased mortality in
10 transiently HS-treated mice is related to differences in blood pressure (BP). BP before and
11 during AngII infusion was continuously measured in conscious mice by radiotelemetry. As
12 expected, AngII treatment rapidly increased the systolic (Fig. 1B, middle) and diastolic BP
13 (Fig. S1A) in both groups. Nevertheless, no differences in the systolic and diastolic BP as
14 well as heart rate between transient HS-treated and control mice were detected (Fig. S1B).

15 Aortic rupture may occur due to AAA or AAD. To investigate whether HS enhances the
16 AngII-induced formation of AAA or AAD, we analyzed the aortic structure by MRI over
17 time. AAA/AAD were detected by a 1.5-fold increase in the outer aortic diameter that is
18 found in both AAA and AAD (Fig. S2A/B). Quantitative assessment of the cumulative
19 incidence showed that AAA/AAD were observed in 63% of mice treated transiently with HS,
20 whereas only 38% of the control mice developed AAA/AAD (Fig. 1B, right, $p < 0.05$).
21 Interestingly, the maximum area of the thrombus in AAD was significantly higher in
22 transiently HS-treated mice compared to control mice (Fig. S3). The number of fibre
23 breakdowns within the aortic wall was nearly 2-fold higher in mice transiently treated with
24 HS compared to control mice (Fig. 1C). Neutrophil elastase exacerbates elastic fiber

1 breakdowns. As shown in Fig. 1D, mRNA levels of neutrophil elastase were elevated in the
2 aortas of AngII-infused mice which were treated transiently with HS compared to
3 hypertensive control mice. After AngII infusion, transiently HS-treated mice showed a larger
4 area of atherosclerotic plaques in the aortic arch than control mice (Fig. 1E). Finally, we
5 analyzed the endothelial function of precontracted aortas. Aortic relaxation induced by
6 carbachol was significantly impaired in the aortas of transiently HS-treated animals compared
7 to control mice (Fig. 1F). Taken together, these observations indicate that HS intake
8 aggravates AngII-induced hypertensive aortic injury in a BP-independent manner.

9

10 **3.2 Salt intake promotes AngII-mediated vascular inflammation**

11 After we have demonstrated that transient HS intake aggravates aortic injury in AngII-infused
12 ApoE^{-/-} mice, we wondered if this is related to vascular inflammation. We utilized combined
13 ¹H/¹⁹F MRI measurements after intravenous injection of perfluorocarbon nanoemulsions
14 (PFCs) for non-invasive assessment of aortic wall inflammation¹⁷. Clear ¹⁹F signals within
15 the aortic wall could be observed in AngII-infused animals of both groups which appeared
16 stronger in the transient HS-treated mice (Fig. 2A). Quantification of the total ¹⁹F signal
17 within the aortic wall revealed a significantly higher ¹⁹F signal on day 4 in mice that received
18 transient HS via the drinking water compared to the control group (Fig. 2B). These findings
19 were supported by subsequent flow cytometric analysis of the number and composition of
20 immune cells within the aortic vessel wall on day 10 of AngII treatment (Fig. 2C, S4 and S5).
21 In accordance with the ¹⁹F data, we found higher numbers of macrophages, monocytes,
22 neutrophils and particularly CD3⁺ T cells in the HS-treated group. Interestingly, we obtained
23 similar results with increased aortic immune cells and ¹⁹F signals for HS-treated mice when
24 we separated the mice into those with or without AAA/AAD (Figure S6). An increased

1 proinflammatory milieu is further substantiated by aortic mRNA expression levels of several
2 inflammatory genes, such as *TNF α* , *iNOS*, and *ICAM-1* that were significantly upregulated in
3 aortas of transiently HS-treated mice compared to aortas from control mice (Figure 2D, upper
4 panel). Noteworthy, also the relative expression of the anti-inflammatory molecules *TGF β* ,
5 *Mgl2*, and *IL10* were elevated in the aortas of transient HS-treated mice (Fig. 2D, lower
6 panel).

7

8 **3.3 High salt leads to subclinical T cell activation prior to AngII treatment**

9 Next, we examined the possibility that salt is sufficient to trigger subclinical vascular injury
10 or a proinflammatory immune phenotype, even in the absence of AngII. MRI measurements
11 of the abdominal area and quantification of the luminal and external cross-section area of the
12 aorta did not show any impact of transient HS intake on aortic anatomy (Fig. 3A).
13 Additionally, the assessment of aortic endothelial function was not affected by transient HS
14 intake (Fig. 3B). Analysis of the aortic immune cells by flow cytometry did not reveal any
15 significant differences in either the number of total CD45⁺ leukocytes, or the total number (or
16 percentage of CD11b) of monocytes, macrophages, and neutrophils (Fig. 3C, Fig. S7C).
17 Interestingly, the number of total CD3⁺ T cells was lower in transient HS-treated mice (Fig.
18 3C, right). However, we found an increased percentage of early activated CD69⁺ CD4⁺ as
19 well as CD8⁺ T cells (Fig. 3D) in transient HS-treated ApoE^{-/-} mice compared to control
20 mice. Moreover, effector memory CD4⁺ (T_{EM} = CD44⁺, CD62L⁻) cells were significantly
21 elevated and naïve CD4⁺ (CD44⁻, CD62L⁺) cells were less abundant in aortas of transient HS-
22 treated mice compared to control mice (Fig. 3E). The proportion of CD4⁺ central memory T
23 cells (T_{CM} = CD44⁺, CD62L⁺; Fig. 3E, middle) and CD8⁺ central memory, effector memory
24 as well as naïve T cells were similar for both groups (Fig. S7A and S8). The relative number

1 of CD4⁺ T cells was significantly higher in the aortas of transient HS mice compared to
2 control mice, whereas for CD8⁺ T cells, no differences were detected between both groups
3 (Fig. S7B and S8). Of note, we did not observe any differences in the number or composition
4 of immune cells or the activation status of T cells in mesenteric lymph nodes two weeks after
5 HS treatment (Fig. S9). Furthermore, we analyzed mRNA expression levels of pro- and anti-
6 inflammatory marker genes in aortas from control and HS-treated mice. Here, transient HS
7 intake did neither affect general pro- or anti-inflammatory markers (Fig. 3F), nor genes
8 associated with T_H1/T_H17 differentiation or M1/M2 polarization of macrophages (Fig. S10).

9

10 **3.4 Transient high salt and AngII elevate aortic effector memory T cells**

11 Since we found a subclinical proinflammatory T cell activation after transient HS intake, we
12 wondered whether this phenotype is further exaggerated by AngII treatment. Flow cytometric
13 analyses of the aorta of mice that were subjected to transient HS and AngII revealed much
14 higher numbers of CD4⁺ and CD8⁺ T cells (Fig. 4A.), as well as frequencies of early
15 activated CD69⁺CD4⁺ T cells (Fig. 4B; 18% ± 2.9 vs. 29% ± 2.3; p<0.05) compared to
16 AngII-infused control mice. The frequencies of CD69⁺CD8⁺ T cells were comparable in both
17 groups (Fig. 4C). Moreover, significantly higher frequencies of CD4⁺ effector memory cells
18 (Fig. 4D) and CD8⁺ central memory cells (Fig. 4E) were detected in the aortas of transient
19 HS-treated mice. Interestingly, the proportion of CD8⁺ T_{EM} and CD4⁺ T_{CM} was similar in the
20 aortic tissue of transient HS-treated and control mice (Fig. 4D/E). No significant differences
21 were found in the frequencies of naïve CD4 and CD8 T cells in the aortas of the two groups
22 (Fig. S11).

23

1 **3.5 The combination of high salt and AngII fosters T_H17 differentiation and T cell-** 2 **mediated endothelial dysfunction**

3 To gain further insights into how transient HS intake affects T cell polarization, mRNA
4 expression levels were assessed in aortas obtained from mice transiently treated with HS and
5 AngII. The HS-treated group displayed increased levels of the T_H1 as well as T_H17 markers
6 *Tbx21*, *ROR γ t* and *IFN γ* compared to corresponding controls (Fig. 5A). *IL17a* was not
7 significantly elevated, but there is a slight trend towards higher expression levels (Fig. 5A,
8 p=0.0919).

9 The number of T cells infiltrating the aorta is very limited, therefore we analyzed the
10 expression of intracellular markers in splenocytes from ApoE^{-/-} mice. Transient HS intake
11 induced a profound IL17⁺ CD4⁺ T_H17 response compared to AngII-infused control mice,
12 whereas levels of IFN γ or TNF α did not differ between transient HS-treated and control mice
13 (Fig. 5B, S12). Moreover, levels of IFN γ ⁺ but not TNF α ⁺ CD8⁺ T cells tend to be higher in
14 AngII-infused mice after transient HS intake indicating enhanced CD8⁺ T_C1 differentiation
15 (Fig. 5C).

16 To assess the effect of HS on activation and differentiation of T cells *in vitro*, we employed T
17 cells from C57BL/6 wild-type mice, because it has been shown that hypercholesterolemia
18 induces a subclinical T cell response in ApoE^{-/-} mice, even in absence of AngII¹⁸. Here,
19 CD3/CD28-activated CD4⁺ and CD8⁺ T cells showed increased secretion of either IL17
20 (CD4⁺ T cells) or IFN γ (CD8⁺ T cells) under HS conditions (Fig. S13), supporting our
21 findings that HS fosters the differentiation into CD4⁺ T_H17 and CD8⁺ T_C1 cells.

22 Chronic HS intake has been shown to aggravate inflammatory responses by reducing the
23 suppressive activity of regulatory T cells (T_{reg})⁹. To investigate the consequences of a
24 transient HS intake, T_{reg} (CD25⁺CD4⁺) isolated from the spleen of mice either treated

1 transiently with HS or tap water were cocultured with activated CD4⁺ T cells from control
2 mice. T_{reg} derived from transient HS or control mice suppressed the proliferation of activated
3 CD4⁺ T cells to a similar extent, suggesting that transient HS intake does not alter the
4 functionality of T_{reg} cells (Fig. 5D, left). These data are supported by intracellular flow
5 cytometry of splenocytes from mice transiently treated with HS and AngII which show a
6 similar amount of FoxP3⁺ CD4⁺ T cells (Fig. 5D, right).

7 Cytokines such as IL17 or TNF α can impair the vascular function of the aorta¹⁹. Therefore,
8 we wondered, if HS treatment exacerbates the release of T cell-derived cytokines that affect
9 endothelial function. Aortas of C57BL/6 wild-type mice were incubated with supernatants of
10 splenic T cells that have been differentiated into either CD4⁺ T_H1, CD4⁺ T_H17, or CD8⁺ T_C1
11 cells in the presence or absence of HS. After 22h of incubation, the effect of the respective
12 supernatant on carbachol-induced endothelial vasorelaxation was analyzed. Here, we
13 observed that the supernatant of CD4⁺ T_H17 and CD8⁺ T_C1 T cells, differentiated under HS
14 conditions, aggravated endothelial dysfunction compared with the supernatant of T cells
15 polarized under normal salt conditions. (Fig. 5E). No difference was observed between the
16 supernatant of HS or control CD4⁺ T_H1 cells on aortic relaxation (Fig. 5E).

17 Since transient HS and AngII treatment results in high numbers of aortic neutrophils and
18 elevated expression of neutrophil elastase, we further investigated the possibility of crosstalk
19 between these cell types. First, we tested if HS-primed T cells stimulate neutrophil migration.
20 Therefore, we cocultured CD4⁺ or CD8⁺ T cells activated with CD3/CD28 in the absence or
21 presence of an additional 40 mM salt, together with neutrophils, and subsequently determined
22 neutrophil migration. We found that neutrophils cocultured with HS-treated CD4⁺ or CD8⁺ T
23 cells displayed a higher ability to migrate towards fMLP (N-Formylmethionyl-leucyl-
24 phenylalanine) than neutrophils cocultured with control CD4⁺ or CD8⁺ T cells (Fig. S14A).
25 In contrast, incubation of neutrophils with HS alone did not affect the migration of these cells

1 (Fig. S14B). Interestingly, treatment of neutrophils with supernatant of activated CD4⁺ or
2 CD8⁺ strongly enhanced neutrophil migration in general (Fig. S15A/B). However, the
3 supernatant of CD4⁺ T cells that were cultured under HS conditions resulted in a slightly
4 reduced neutrophil migration compared to controls cultured under normal salt (Fig. S15A),
5 whereas the supernatant of CD8⁺ activated under HS or normal salt stimulated neutrophil
6 migration to a similar extent (Fig. S15B). Next, we investigated the effect of these cytokines
7 on neutrophil migration. We found that IFN γ and IL17, either separately or in combination,
8 did not promote neutrophil migration towards fMLP (Fig. S16).

9 Finally, we investigated whether T cells modulate the ability of neutrophils to undergo
10 NETosis (NET = Neutrophil extracellular traps), that has been linked to endothelial
11 dysfunction and vascular inflammation²⁰. Bone marrow-derived neutrophils, cocultured with
12 CD3/CD28 activated and HS-treated CD4⁺ T cells or CD4⁺ T cells cultivated under normal
13 salt concentrations showed a similar level of NET-formation (Fig. S17).

14

1 **4. Discussion**

2 Salt overconsumption is an important factor in the development and progression of CVD
3 while the reduction in HS intake decreases cardiovascular morbidity and mortality in
4 hypertensive patients²¹. Recent data have shown that salt not only increases BP but also shifts
5 immune responses to a proinflammatory phenotype²². However, it is still unclear whether
6 immune response modulation by HS can affect cardiovascular diseases.

7 In the present study, we investigated the influence of transient dietary HS intake on the
8 development and progression of AngII-induced hypertensive vascular injury in ApoE^{-/-} mice.
9 First, mice were transiently treated for two weeks with HS via drinking water, followed by a
10 washout period with normal tap water for an additional week. This transient HS intake did
11 not induce aortic disease but induced a subclinical aortic immune response with increased
12 activated and memory aortic CD4⁺ T cells. Subsequent AngII-induced hypertension caused
13 an exaggerated vascular inflammation with increased aortic immune cells and a more
14 pronounced CD4⁺ T_{EM}, T_H17 as well as a CD8⁺ Tc1 T cell response. Additionally, aortic
15 injury characterized by more severe AAA/AAD, endothelial dysfunction, and atherosclerosis
16 was also increased after transient HS and AngII. Thus, we conclude that hypertensive aortic
17 injury can be exacerbated by transient HS intake and that this is rather driven by
18 immunological effects and not by differences in BP.

19 **Transient HS- and AngII-induced CD4⁺ T_{EM} and T_H17 cells mediate aortic damage**

20 After 10 days of AngII infusion, the aortas of transiently HS-treated mice displayed a
21 significantly elevated number of early activated CD4⁺/CD69⁺ T cells as well as effector
22 memory CD4⁺ T cells (T_{EM}) compared to control mice. Higher numbers of aortic immune
23 cells were not only observed in mice with AAA/AAD, but also in mice without AAA/AAD.
24 Importantly, there was no difference in the BP between the two groups which indicates that

1 the accumulation of activated and memory T cells within the aorta is not due to higher BP in
2 transiently HS-treated mice. Several studies have shown that high BP can induce the
3 generation of effector and memory T cells in the blood, vasculature, and kidney²³.
4 Particularly repeated hypertensive stimuli such as treatment with the NO-synthase inhibitor
5 L-NAME followed by a washout period and HS (4 % NaCl) induced high numbers of CD4⁺
6 and CD8⁺ T_{EM} cells within the kidney and the bone marrow²⁴. In our study, we observed that
7 AngII-infusion after transient HS intake enhances the number of activated T cells and T_{EM}
8 within the aorta compared to AngII without a prior transient HS intake. Additionally, Itani et
9 al.²⁴ found that effector memory T cells within the kidney are a major source of IFN γ which
10 is known to induce hypertensive kidney damage²⁵. We also found high levels of IFN γ in the
11 aorta, but we did not observe any differences in BP response.

12 Apart from different treatment durations, one explanation for the disparate results could be
13 that Itani et al. used C57BL/6 mice and that the ApoE^{-/-} mice we used in our experiments are
14 more prone to generate aortic memory T cells²⁶. This assumption is supported by the
15 observation that naïve T cells can directly differentiate within the aorta of atherosclerotic
16 ApoE^{-/-} mice and therefore show high numbers of activated and effector/memory CD4⁺ T
17 cells²⁷. Another possibility is that transient HS intake pre-stimulates T cells more efficiently,
18 and that AngII-induced hypertension then promotes the proliferation and activation of these
19 primed T cells. This hypothesis is in line with our observations that HS intake without AngII
20 is sufficient to induce the accumulation of CD4⁺ CD69⁺ and CD4⁺ memory T cells in the
21 aorta of ApoE^{-/-} mice as a sign of a subclinical vascular immune response.

22 After transient HS intake and AngII, we observed significantly higher aortic levels of the key
23 transcription factor for the generation of T_H17 cells, ROR γ t, as well as elevated levels of
24 IL17. Moreover, we found an increased number of splenic T_H17 CD4⁺ T cells, indicating that
25 transient HS and AngII trigger the formation of T_H17 cells. These findings are in agreement

1 with previous studies that have clearly shown that HS promotes the differentiation of naïve T
2 cells into T_H17 cells that exacerbate experimentally induced encephalomyelitis (EAE)^{6,7}. The
3 relevance of this observation for the development of cardiovascular damage is supported by
4 the fact that the supernatant of CD4⁺ T_H17 cells, differentiated under HS conditions, impairs
5 the endothelial function of aortas to a higher degree than T_H17 cells differentiated under
6 normal salt conditions. Most likely, this is due to an increased release of IL17, which is
7 sufficient to aggravate endothelial dysfunction^{19,28-30}. Furthermore, IL17 enhances neutrophil
8 recruitment to inflammatory lesions by activation of endothelial cells resulting in increased
9 expression of adhesion markers such as ICAM-1³¹. In agreement with this, we found higher
10 expression levels of ICAM-1, a five-fold increased number of neutrophils in aortas of HS-
11 treated mice, and that IL17 alone does not stimulate neutrophil chemotaxis. This suggests that
12 IL17-secreting T_H17 cells may aggravate aortic inflammation by enhancing endothelial
13 dysfunction and stimulation of endothelial cells that increases the infiltration of neutrophils
14 into the aorta. Thus, it is plausible, that the second hypertensive hit, in our case AngII,
15 triggers an enhanced differentiation of these pre-stimulated T cells into T_H17 T cells, which
16 then causes increased vascular inflammation and vascular injury.

17 Although we found an increased expression of the T_H1 markers *Tbx21* and *IFN*γ in the aorta,
18 we did not detect an effect of transient HS intake on T_H1 CD4⁺ T cell differentiation and
19 endothelial function *ex vivo*. IFNγ did also not foster neutrophil migration towards fMLP.
20 This observation does not rule out a role for T_H1 T cells in the development of aortic injury³²
21 but suggests that transient HS intake does not induce polarization of naïve murine CD4⁺ T
22 cells into T_H1 CD4⁺ T cells, thereby impairing aortic function. Similarly, *in vitro* data show
23 that polarization of naïve T cells into T_H1 CD4⁺ T cells under HS concentrations reduces
24 IFN-γ production³³.

25

1 **HS-mediated vascular damage is not related to regulatory T cells**

2 Recently, we have shown that HS intake affects the functionality of T_{regs} ⁹. Thus, it was
3 plausible to investigate whether an enhanced inflammatory response in the aorta of AngII-
4 infused mice could be due to impaired functionality of T_{regs} triggered by a transient HS
5 intake. In the present study, we did not observe any differences in the number of splenic
6 $CD25^+$ T cells between the two groups after AngII treatment. Besides the total amount, the
7 biological function of T_{regs} cells is largely responsible for the modulation of inflammatory
8 processes. However, our T_{regs} suppression assay performed in coculture experiments with
9 isolated T_{regs} from transient HS-treated mice and control animals did not provide evidence for
10 impaired suppressive activity on the proliferation of activated $CD4^+$ T cells. This seems to be
11 in contradiction to previous investigations where we and others have shown that HS can
12 indeed impair T_{reg} function by perturbation of mitochondrial function or the induction of
13 $IFN\gamma$ expression^{9,34,35}. These differences could be due to the genetic background of the
14 animals, the treatment, and the disease model. Interestingly, in the aortas of transiently HS
15 and AngII-treated mice, we found increased expression levels of anti-inflammatory cytokines
16 such as IL10 and $TGF\beta$ suggesting a potential T_{reg} -independent enhanced compensatory
17 capacity in these mice to reduce the aggravated AngII-induced vascular damage^{28,36}.
18 Therefore, we hypothesize that transient HS followed by AngII-induces excessive aortic
19 inflammation and damage through a mechanism that is not related to a decreased
20 functionality of T_{regs} .

21 **Impact of $CD8^+$ T_C1 cells and a neutrophil T cell crosstalk**

22 Mice treated transiently with HS followed by AngII showed more $CD8^+$ T cells in the aorta
23 compared to control mice. Additionally, the supernatant of $CD8^+$ T_C1 cells activated by
24 $CD3/CD28$ under HS significantly impaired aortic endothelial function. Intracellular cytokine

1 levels of splenic CD8⁺ T cells showed a trend towards a higher expression of IFN γ and
2 similar results were obtained by *in vitro* activation of CD8⁺ T cells under HS conditions,
3 indicating that HS promotes the differentiation into a CD8⁺ T_C1 phenotype. In contrast to
4 CD4⁺ T cells, a direct impact of HS on the activation and differentiation of CD8⁺ T cells have
5 not been investigated yet. However, this mechanism seems plausible since a recent study
6 showed that serum glucocorticoid kinase 1 (SGK1), which mediates HS-dependent T cell
7 differentiation³⁷, is expressed in CD8⁺ T cells and that SGK1 expression modulates the
8 differentiation of CD8⁺ memory cells³⁸. Furthermore, our results showing that enhanced
9 CD8⁺ T_C1 cell differentiation may be responsible for the progression of vascular
10 inflammation and injury are in line with several studies describing an important role of CD8⁺
11 effector T cells in the pathogenesis of vascular inflammation, atherosclerosis and AAA
12 formation^{39,40}.

13 Another finding of our study was that HS can modulate the crosstalk between T cells and
14 neutrophil granulocytes. *In vitro* coculture experiments with HS-activated CD8⁺ and CD4⁺
15 revealed an enhanced migration of neutrophils towards fMLP, whereas HS alone did not have
16 any effect. Supernatants from activated CD4⁺ and CD8⁺ cells strongly influenced neutrophil
17 migration in general, but there was no difference between the supernatant from HS or control
18 cells. Furthermore, IFN γ did not elevate the migration of bone marrow neutrophils towards
19 fMLP. This suggests that T cell-derived chemokines stimulate the chemotaxis of neutrophils,
20 but additional signals that are mediated via direct cell-cell contact are responsible for the
21 increased neutrophil migration after coculture with HS-activated T cells. An interesting
22 question is where neutrophils and T cells meet and how this cell-cell contact leads to
23 increased chemotactic activity. Recently it has been found that neutrophils recirculate through
24 lymph nodes where they can interact with T cells^{41,42} and this interaction may increase
25 neutrophil migration into the aorta. However, additional studies are necessary to further

1 unravel how high levels of dietary salt are transduced and modify immune responses. It is
2 tempting to speculate that endothelial cells and the surrounding microenvironment play an
3 important role because they have been described to serve as vascular salt sensors and the
4 endothelial surface layer is potentially involved in local sodium storage⁴³. This particular
5 environment might promote the skewing of inflammatory T-cell responses.

6 Taken together, our results show that HS has a strong BP-independent immunological impact
7 on the development and progression of hypertensive aortic inflammation and associated
8 aortic diseases such as aortic rupture, AAA/AAD, or atherosclerosis. Mechanistically, we
9 hypothesize that transient HS induces a subclinical aortic immune response with increased
10 amounts of CD69⁺ CD4⁺ and T_{EM} cells. Subsequently, despite no differences in BP, AngII-
11 induced hypertension then shifts the aortic CD4⁺ T cell response towards a pronounced
12 effector memory and T_H17 direction that results in an excessive immune reaction with severe
13 endothelial dysfunction and the infiltration of neutrophils, monocytes/macrophages and CD8⁺
14 T_C1 cells compared to AngII-infused control mice. Our observations are clinically relevant
15 because there are two billion hypertensive individuals worldwide and repetitive high salt
16 consumption is a global phenomenon. Thus, if HS triggers the formation of aortic memory T
17 cells that are reactivated even in response to hypertension, then this could lead to an
18 avoidable increase in vascular damage.

19 There are multiple ways how salt affects the phenotype and function of immune cells, like T
20 cells or neutrophils. Besides direct effects on the activation and differentiation of T cells, HS
21 can also indirectly influence immune responses for example by altering the gut microbiome.
22 Wilck and colleagues have shown that high salt intake decreases *lactobacillus murinus* in the
23 gut, which leads to a lower metabolization of fecal tryptophan to indole-3-lactic and to an
24 increased proinflammatory T_H17 T cell response⁸. Furthermore, high salt has also been
25 shown to affect sympathetic nerve activity, especially in salt-sensitive animals⁴⁴. Increased

1 splenic sympathetic nerve activity can induce a proinflammatory immune response by
2 releasing placental growth factor (PIGF)⁴⁵⁻⁴⁷. Additionally, the sympathetic nervous system
3 can alter T cell priming and homing in the bone marrow⁴⁸. Based on these studies, it could be
4 possible that the findings observed in this study are driven by a complex neuronal-
5 splenic/bone marrow-artery cross-talk.

6

7 **5. Perspectives**

8 High salt (HS) intake is a hallmark of western diets and an important risk factor for the
9 development and progression of cardiovascular diseases, because HS does not only affect the
10 blood pressure, but does also impact immune responses. Furthermore, it has been shown that
11 transient HS episodes can lead to elevated blood pressure even long-term after normalization
12 of the salt intake. This so-called salt memory phenomenon is based on various not yet fully
13 elucidated mechanisms, including immune cell responses. Considering that there are two
14 billion people with hypertension worldwide and repeated high salt consumption is a global
15 phenomenon, HS-induced polarization of memory T cells could have a major impact on
16 cardiovascular disease. Therefore, constant reduction of salt intake, particularly in
17 hypertensive high-risk patients, could strongly reduce the vascular disease burden. However,
18 future studies are needed to precisely decipher the pathophysiological mechanisms, including
19 interorganic communication, in order to identify the patients with the highest risk profile and
20 open up new perspectives for therapeutic strategies.

21

22

1 **6. Acknowledgements**

2 We thank Blanka Duvnjak und Nicola Kuhr for technical assistance.

3

4 **7. Author contributions**

5 Drs Müller, Temme and Stegbauer designed the study. Argov, Arifaj, Feige as well as Drs
6 Yakoub, Rahman, Alter, Hering, Kantauskaite and Meister performed experiments in ApoE^{-/-}
7 mice and analyzed and interpreted the data. Kleinmann, Hoffe, Kluczny, Reidel as well as
8 Drs Yakoub, Rahman, Bouvain and Nederlof performed *in vitro* experiments in T cells and
9 neutrophils and analyzed and interpreted the data. Drs Jantsch, Meister, Rump, Flögel and
10 Kleinewietfeld helped with data analysis, interpretation and writing. Drs Temme,
11 Kleinewietfeld, Rump and Stegbauer wrote the manuscript with input from all authors.

12

13 **8. Sources of funding**

14 This work was supported by the German Research Foundation (CRC 1116 to U.F.; CRC 259
15 to U.F.; CRC1470 A06 to D.N.M.; FL303/6-1/2 to U.F.; INST 208/764-1 FUGG to U.F.;
16 TE1209/1-1/2 to S.T.; IRTG1902 to J.S., STE2042/2-1 to J.S.). D.N.M. was supported by the
17 Deutsches Zentrum für Herz-Kreislauf-Forschung (DZHK, 81Z0100106).

18 M.K. was supported by the European Research Council (ERC) under the European Union's
19 Horizon 2020 research and innovation program (Project ID 640116), by a SALK-grant from
20 the government of Flanders, by an Odysseus-grant (Project ID G0G1216FWO) and senior
21 research project (Project ID G080121N) of the FWO and by a BOF grant (ADMIRE, Project
22 ID 21GP17BOF) from Hasselt University.

1

2

3 **9. Disclosures**

4 None

5

6 **10. Supplemental Material:**

7 - Expanded Methods: SM1-SM12

8 - References

9 - Tables: S1-S3

10 - Figures S1-S17

11

12

13

1 11. References

- 2 1. MacGregor GA, Wardener HE de. Salt, Diet and Health. Cambridge University Press;
3 1998.
- 4 2. Mozaffarian D, Fahimi S, Singh GM, Micha R, Khatibzadeh S, Engell RE, Lim S,
5 Danaei G, Ezzati M, Powles J. Global Sodium Consumption and Death from
6 Cardiovascular Causes. *N Engl J Med*. 2014;371:624–634.
- 7 3. Whelton PK, Appel LJ, Sacco RL, Anderson CAM, Antman EM, Campbell N, Dunbar
8 SB, Frohlich ED, Hall JE, Jessup M, et al. Sodium, Blood Pressure, and Cardiovascular
9 Disease. *Circulation*. 2012;126:2880–2889.
- 10 4. Wenstedt EF, Verberk SG, Kroon J, Neele AE, Baardman J, Claessen N, Pasaoglu ÖT,
11 Rademaker E, Schrooten EM, Wouda RD, de Winther MP, Aten J, Vogt L, Van den
12 Bossche J. Salt increases monocyte CCR2 expression and inflammatory responses in
13 humans. *JCI Insight*. 2019;4:130508.
- 14 5. Ruggeri Barbaro N, Van Beusecum J, Xiao L, do Carmo L, Pitzer A, Loperena R, Foss
15 JD, Elijovich F, Laffer CL, Montaniel KR, et al. Sodium activates human monocytes via
16 the NADPH oxidase and isolevuglandin formation. *Cardiovasc Res*. 2021;117:1358–
17 1371.
- 18 6. Wilck N, Matus MG, Kearney SM, Olesen SW, Forslund K, Bartolomaeus H, Haase S,
19 Mähler A, Balogh A, Markó L, et al. Salt-responsive gut commensal modulates TH17
20 axis and disease. *Nature*. 2017;551:585–589.
- 21 7. Kleinewietfeld M, Manzel A, Titze J, Kvakan H, Yosef N, Linker RA, Muller DN,
22 Hafler DA. Sodium chloride drives autoimmune disease by the induction of pathogenic
23 TH17 cells. *Nature*. 2013;496:518–522.
- 24 8. Teixeira DE, Peruchetti DB, Souza MC, das Graças Henriques MG, Pinheiro AAS,
25 Caruso-Neves C. A high salt diet induces tubular damage associated with a pro-
26 inflammatory and pro-fibrotic response in a hypertension-independent manner. *Biochim*
27 *Biophys Acta BBA - Mol Basis Dis*. 2020;1866:165907.
- 28 9. Côte-Real BF, Hamad I, Arroyo Hornero R, Geisberger S, Roels J, Van Zeebroeck L,
29 Dyczko A, van Gisbergen MW, Kurniawan H, Wagner A, et al. Sodium perturbs
30 mitochondrial respiration and induces dysfunctional Tregs. *Cell Metab*. 2023;35:299-
31 315.e8.
- 32 10. Geisberger S, Bartolomaeus H, Neubert P, Willebrand R, Zasada C, Bartolomaeus T,
33 McParland V, Swinnen D, Geuzens A, Maifeld A, et al. Salt Transiently Inhibits
34 Mitochondrial Energetics in Mononuclear Phagocytes. *Circulation*. 2021;144:144–158.
- 35 11. Zhang W-C, Zheng X-J, Du L-J, Sun J-Y, Shen Z-X, Shi C, Sun S, Zhang Z, Chen X,
36 Qin M, Liu X, et al. High salt primes a specific activation state of macrophages, M(Na).
37 *Cell Res*. 2015;25:893–910.
- 38 12. Machnik A, Neuhofer W, Jantsch J, Dahlmann A, Tammela T, Machura K, Park J-K,
39 Beck F-X, Müller DN, Derer W, et al. Macrophages regulate salt-dependent volume and

- 1 blood pressure by a vascular endothelial growth factor-C-dependent buffering
2 mechanism. *Nat Med.* 2009;15:545–552.
- 3 13. Libby P. The changing landscape of atherosclerosis. *Nature.* 2021;592:524–533.
- 4 14. Yuan Z, Lu Y, Wei J, Wu J, Yang J, Cai Z. Abdominal Aortic Aneurysm: Roles of
5 Inflammatory Cells. *Front Immunol.* 2020;11:609161.
- 6 15. Golledge J, Hankey GJ, Yeap BB, Almeida OP, Flicker L, Norman PE. Reported High
7 Salt Intake Is Associated with Increased Prevalence of Abdominal Aortic Aneurysm and
8 Larger Aortic Diameter in Older Men. *PLOS ONE.* 2014;9:e102578.
- 9 16. Zhao X, Yang X, Zhang X, Li Y, Zhao X, Ren L, Wang L, Gu C, Zhu Z, Han Y.
10 Dietary salt intake and coronary atherosclerosis in patients with prehypertension. *J Clin*
11 *Hypertens Greenwich Conn.* 2014;16:575–580.
- 12 17. Temme S, Yakoub M, Bouvain P, Yang G, Schrader J, Stegbauer J, Flögel U. Beyond
13 Vessel Diameters: Non-invasive Monitoring of Flow Patterns and Immune Cell
14 Recruitment in Murine Abdominal Aortic Disorders by Multiparametric MRI. *Front*
15 *Cardiovasc Med.* 2021;8:1421.
- 16 18. Dimayuga PC, Zhao X, Yano J, Lio WM, Zhou J, Mihailovic PM, Cercek B, Shah PK,
17 Chyu K. Identification of apoB-100 Peptide-Specific CD8+ T Cells in Atherosclerosis. *J*
18 *Am Heart Assoc.* 2017;6:e005318.
- 19 19. Nguyen H, Chiasson VL, Chatterjee P, Kopriva SE, Young KJ, Mitchell BM.
20 Interleukin-17 causes Rho-kinase-mediated endothelial dysfunction and hypertension.
21 *Cardiovasc Res.* 2013;97:696–704.
- 22 20. Qi H, Yang S, Zhang L. Neutrophil Extracellular Traps and Endothelial Dysfunction in
23 Atherosclerosis and Thrombosis. *Front Immunol.* 2017;8:928.
- 24 21. Neal B, Wu Y, Feng X, Zhang R, Zhang Y, Shi J, Zhang J, Tian M, Huang L, Li Z, Yu
25 Y, et al. Effect of Salt Substitution on Cardiovascular Events and Death. *N Engl J Med.*
26 2021;385:1067–1077.
- 27 22. Rucker AJ, Rudemiller NP, Crowley SD. Salt, Hypertension, and Immunity. *Annu Rev*
28 *Physiol.* 2018;80:283–307.
- 29 23. Itani HA, Harrison DG. Memories that last in hypertension. *Am J Physiol-Ren Physiol.*
30 2015;308:F1197–F1199.
- 31 24. Itani HA, Xiao L, Saleh MA, Wu J, Pilkinton MA, Dale BL, Barbaro NR, Foss JD,
32 Kirabo A, Montaniel KR, et al. CD70 Exacerbates Blood Pressure Elevation and Renal
33 Damage in Response to Repeated Hypertensive Stimuli. *Circ Res.* 2016;118:1233–1243.
- 34 25. Kamat NV, Thabet SR, Xiao L, Saleh MA, Kirabo A, Madhur MS, Delpire E, Harrison
35 DG, McDonough AA. Renal transporter activation during angiotensin-II hypertension is
36 blunted in interferon- γ -/- and interleukin-17A-/- mice. *Hypertens Dallas Tex 1979.*
37 2015;65:569–576.

- 1 26. Ammirati E, Cianflone D, Vecchio V, Banfi M, Vermi AC, De Metrio M, Grigore L,
2 Pellegatta F, Pirillo A, Garlaschelli K, Manfredi AA, Catapano AL, Maseri A, Palini
3 AG, Norata GD. Effector Memory T cells Are Associated With Atherosclerosis in
4 Humans and Animal Models. *J Am Heart Assoc.* 1:e000125.
- 5 27. MacRitchie N, Grassia G, Noonan J, Cole JE, Hughes CE, Schroeder J, Benson RA,
6 Cochain C, Zerneck A, Guzik TJ, Garside P, Monaco C, Maffia P. The aorta can act as
7 a site of naïve CD4+ T-cell priming. *Cardiovasc Res.* 2020;116:306–316.
- 8 28. Bartolomaeus H, Balogh A, Yakoub M, Homann S, Markó L, Höges S, Tsvetkov D,
9 Krannich A, Wundersitz S, Avery EG, et al. Short-Chain Fatty Acid Propionate Protects
10 From Hypertensive Cardiovascular Damage. *Circulation.* 2019;139:1407–1421.
- 11 29. Huppert J, Closhen D, Croxford A, White R, Kulig P, Pietrowski E, Bechmann I,
12 Becher B, Luhmann HJ, Waisman A, Kuhlmann CRW. Cellular mechanisms of IL-17-
13 induced blood-brain barrier disruption. *FASEB J.* 2010;24:1023–1034.
- 14 30. Kudo M, Melton AC, Chen C, Engler MB, Huang KE, Ren X, Wang Y, Bernstein X, Li
15 JT, Atabai K, Huang X, Sheppard D. IL-17A produced by $\alpha\beta$ T cells drives airway
16 hyper-responsiveness in mice and enhances mouse and human airway smooth muscle
17 contraction. *Nat Med.* 2012;18:547–554.
- 18 31. Roussel L, Houle F, Chan C, Yao Y, Bérubé J, Olivenstein R, Martin JG, Huot J, Hamid
19 Q, Ferri L, Rousseau S. IL-17 Promotes p38 MAPK-Dependent Endothelial Activation
20 Enhancing Neutrophil Recruitment to Sites of Inflammation. *J Immunol.*
21 2010;184:4531–4537.
- 22 32. Chen J, Xiang X, Nie L, Guo X, Zhang F, Wen C, Xia Y, Mao L. The emerging role of
23 Th1 cells in atherosclerosis and its implications for therapy. *Front Immunol* [Internet].
24 2023 [cited 2023 Nov 22];13. Available from:
25 <https://www.frontiersin.org/articles/10.3389/fimmu.2022.1079668>
- 26 33. Matthias J, Maul J, Noster R, Meinel H, Chao Y-Y, Gerstenberg H, Jeschke F, Gasparoni
27 G, Welle A, Walter J, Nordström K, et al. Sodium chloride is an ionic checkpoint for
28 human TH2 cells and shapes the atopic skin microenvironment. *Sci Transl Med.*
29 2019;11:eaau0683.
- 30 34. Hernandez AL, Kitz A, Wu C, Lowther DE, Rodriguez DM, Vudattu N, Deng S, Herold
31 KC, Kuchroo VK, Kleinewietfeld M, Hafler DA. Sodium chloride inhibits the
32 suppressive function of FOXP3+ regulatory T cells. *J Clin Invest.* 2015;125:4212–4222.
- 33 35. Yang YH, Istomine R, Alvarez F, Al-Aubodah T-A, Shi XQ, Takano T, Thornton AM,
34 Shevach EM, Zhang J, Piccirillo CA. Salt Sensing by Serum/Glucocorticoid-Regulated
35 Kinase 1 Promotes Th17-like Inflammatory Adaptation of Foxp3+ Regulatory T Cells.
36 *Cell Rep.* 2020;30:1515-1529.e4.
- 37 36. Mallat Z, Heymes C, Ohan J, Faggin E, Lesèche G, Tedgui A. Expression of
38 interleukin-10 in advanced human atherosclerotic plaques: relation to inducible nitric
39 oxide synthase expression and cell death. *Arterioscler Thromb Vasc Biol.* 1999;19:611–
40 616.

- 1 37. Müller DN, Wilck N, Haase S, Kleinewietfeld M, Linker RA. Sodium in the
2 microenvironment regulates immune responses and tissue homeostasis. *Nat Rev*
3 *Immunol.* 2019;19:243–254.
- 4 38. Patel CH, Heikamp EB, Xu W, Sun I-H, Oh M-H, Sun I-M, Wen J, Tam AJ, Blosser
5 RL, Powell JD. Cutting Edge: mTORC2 Regulates CD8+ Effector and Memory T Cell
6 Differentiation through Serum and Glucocorticoid Kinase 1. *J Immunol.*
7 2022;209:2287–2291.
- 8 39. Schäfer S, Zerneck A. CD8+ T Cells in Atherosclerosis. *Cells.* 2021;10:37.
- 9 40. Lv B-J, Li J, Cheng X. T lymphocytes and aortic aneurysms. *Sci China Life Sci.*
10 2014;57:795–801.
- 11 41. Bogoslawski A, Wijeyesinghe S, Lee W-Y, Chen C-S, Alanani S, Jenne C, Steeber DA,
12 Scheiermann C, Butcher EC, Masopust D, Kubes P. Neutrophils Recirculate through
13 Lymph Nodes to Survey Tissues for Pathogens. *J Immunol.* 2020;204:2552–2561.
- 14 42. Lok LSC, Dennison TW, Mahbubani KM, Saeb-Parsy K, Chilvers ER, Clatworthy MR.
15 Phenotypically distinct neutrophils patrol uninfected human and mouse lymph nodes.
16 *Proc Natl Acad Sci.* 2019;116:19083–19089.
- 17 43. Miyauchi H, Geisberger S, Luft FC, Wilck N, Stegbauer J, Wiig H, Dechend R, Jantsch
18 J, Kleinewietfeld M, Kempa S, Müller DN. Sodium as an Important Regulator of
19 Immunometabolism. *Hypertension.* 2023; 81:426-435.
- 20 44. Simmonds SS, Lay J, Stocker SD. Dietary Salt Intake Exaggerates Sympathetic
21 Reflexes and Increases Blood Pressure Variability in Normotensive Rats. *Hypertension.*
22 2014;64:583–589.
- 23 45. Perrotta M, Lori A, Carnevale L, Fardella S, Cifelli G, Iacobucci R, Mastroiacovo F,
24 Iodice D, Pallante F, Storto M, Lembo G, Carnevale D. Deoxycorticosterone acetate-salt
25 hypertension activates placental growth factor in the spleen to couple sympathetic drive
26 and immune system activation. *Cardiovasc Res.* 2018;114:456–467.
- 27 46. Carnevale D, Pallante F, Fardella V, Fardella S, Iacobucci R, Federici M, Cifelli G, De
28 Lucia M, Lembo G. The angiogenic factor PlGF mediates a neuroimmune interaction in
29 the spleen to allow the onset of hypertension. *Immunity.* 2014;41:737–752.
- 30 47. Mohanta SK, Peng L, Li Y, Lu S, Sun T, Carnevale L, Perrotta M, Ma Z, Förster B,
31 Stanic K, et al. Neuroimmune cardiovascular interfaces control atherosclerosis. *Nature.*
32 2022;605:152–159.
- 33 48. Xiao L, do Carmo LS, Foss JD, Chen W, Harrison DG. Sympathetic Enhancement of
34 Memory T-Cell Homing and Hypertension Sensitization. *Circ Res.* 2020;126:708–721.

35

1 **12. Novelty and Relevance**

2 **What is new?**

- 3 • Transient high salt intake triggers a subclinical vascular immune response.
- 4 • Transient high salt intake exacerbates hypertensive aortic injury without affecting
- 5 blood pressure.

6 **What is relevant?**

- 7 • Transient high salt intake acts as a predisposing factor to cause more severe
- 8 hypertension-induced T_H17 and T_C1 polarization and aortic injury

9 **Clinical / Pathophysiological implications?**

- 10 • In hypertensive individuals, even a transient high salt intake may be sufficient to
- 11 trigger a proinflammatory immune response that exacerbates hypertensive vascular
- 12 damage.
- 13 • Reduction of salt intake could mitigate the incidence of atherosclerosis and aortic
- 14 aneurysms, especially in hypertensive patients.

15

16

17 **13. Figure Legends**

18 **Figure 1: Transient high salt and AngII treatment enhance aortic tissue damage: A)**

19 Schematic overview of the experimental setup. Apolipoprotein E-deficient mice (ApoE^{-/-})
20 were treated with 1% NaCl in the drinking water (or tap water as control) for 14 days,
21 followed by one week of normal tap water (HS = transient high salt). Osmotic minipumps
22 with AngII were subcutaneously implanted and mice were monitored by magnetic resonance

1 imaging (MRI) for 10 days. **B) Left:** Survival curve of AngII-infused mice treated either
2 transiently with HS (red) tap water (control, black). Control n=32, HS n=25. *p<0.05, by log-
3 rank test. **Middle:** Telemetric measurements of systolic blood pressure (BP) in mice before
4 and after implantation of AngII minipumps. The dashed line indicates the day of minipump
5 implantation. Control and HS n=3-5. Not significant, by 2-way ANOVA. **Right:** Cumulative
6 incidence of the formation of abdominal aortic aneurysms (AAA) or abdominal aortic
7 dissections (AAD). Control n=29, Salt n=21. *p<0.05, by log-rank test. **C)** Histological
8 determination of elastic fiber breakdowns in the aortic wall, by staining with Movat's
9 pentachrome staining. Arrows in the magnification highlight the position of elastic fiber
10 breaks. Right: Quantification of the average number of fiber breakdowns in three transverse
11 sections. Control n=5, HS n=6. *p<0.05, by unpaired, two-tailed t-test. **D)** Relative mRNA
12 expression levels of neutrophil elastase in aortas obtained from of AngII-infused HS or
13 control treated ApoE^{-/-} mice. A.U. = arbitrary units; Control n=6, HS n=8. ***p<0.001, by
14 unpaired, one-tailed t-test. **E)** Assessment of atherosclerotic plaques in the aortic arch. Left:
15 Oil red staining of the aortic arch; arrows indicate the position of atherosclerotic lesions.
16 Right: Quantification of the atherosclerotic area. Control and HS n=8. *p<0.05, by two-tailed,
17 unpaired t-test with Welch's correction. **F)** Vessel myography of excised aortas. Control n=5,
18 HS n=4. *p<0.05, **p<0.01 by 2-way ANOVA followed by Sidak's multiple comparison
19 test.

20

21 **Figure 2: Transient high salt intake aggravates AngII-induced aortic inflammation: A)**

22 Axial ¹H/¹⁹F MRI images of the abdominal area of mice that received high salt (1 %) via the
23 drinking water (HS) or tap water (as control), followed by one week with normal water and
24 AngII treatment for additional ten days. Upper: Anatomical axial cross-section ¹H images,
25 middle: Corresponding ¹⁹F images, bottom: Overlay of ¹H/¹⁹F data. A magnification of the

1 aortic area is shown on the right. Scale bars = 1 mm and 2 mm for the magnification. The ^{19}F
2 signals of the liver and spleen were faded out to enhance the clarity of the ^{19}F signals in the
3 aortic vessel wall. **B)** Quantification of the total ^{19}F signal intensity in the aortic wall. ^{19}F data
4 of the HS and the control group for the time points (day 2, day 4, and day 7) were statistically
5 analyzed with a two-tailed Mann-Whitney U test (* $p < 0.05$). The n-number of the animals
6 decreased over time due to aortic rupture (see Fig.1). Control/HS Day 0: n=14/14, Day 2:
7 14/12, Day 7: 12/8. **C) Left:** Zebra plots that show aortic monocytes, macrophages and
8 neutrophils (upper) and CD3^+ T cells (lower) of control (left) or HS treated ApoE $^{-/-}$ mice
9 (right) **Right:** Corresponding quantitative analysis of the cell counts of macrophages,
10 monocytes, neutrophils, and CD3^+ T cells in the aortic wall of ApoE $^{-/-}$ mice, determined by
11 flow cytometry. Control n=9-10, HS n=11. * $p < 0.05$, ** $p < 0.01$ by two-tailed Mann-Whitney
12 U test. **D)** Relative mRNA-expression levels in arbitrary units (A.U.) of inflammatory markers
13 in aortas derived from control animals (black) or mice subjected to HS (red). The expression
14 of mRNA is normalized to the house keeping gene GAPDH. Control n=6-7, HS n=7-8.
15 * $p < 0.05$, ** $p < 0.01$, *** $p < 0.001$ by one-tailed t-test with Welch's correction or Mann-
16 Whitney U test.

17

18 **Figure 3: Transient high salt intake (HS) without AngII induces subclinical T cell**
19 **activation: A) Left:** Anatomical (upper) and angiographic axial MRI cross-section images.
20 Yellow arrow = aorta, blue arrow = vena cava. Scale bars = 1 mm. **Right:** Quantitative
21 analysis of the maximum cross-section area of the external and luminal parts of the aorta.
22 Control/HS n=10. Statistical analysis by one-tailed, unpaired t-test with/without Welch's
23 correction. **B)** Vessel myography of excised aortas from control mice (grey) or HS-treated
24 animals (green). Control n=2, HS n=3. Not significant, by 2-way ANOVA. **C)** Flow
25 cytometric analysis of total aortic immune cells (CD45^+), monocytes, macrophages and

1 neutrophil granulocytes of ApoE^{-/-} mice treated with or without transient high salt (HS).
2 Control n=9, HS n=10. Statistical analysis: One-tailed, unpaired t-test or Mann-Whitney U
3 test. **D)** Percentage of cells expressing the early activation marker CD69 on CD4⁺ (left) and
4 CD8⁺ (right) T cells. Control n=9, HS n=9-10. *p<0.05 by one-tailed, unpaired t-test with
5 Welch's correction. **E)** Flow cytometric analysis of CD4⁺ T cells derived from the aortas of
6 ApoE^{-/-} mice control animals and mice subjected to HS. Effector memory T cells (T_{EM}) =
7 CD44⁺/CD62L⁻; Central memory T cells (T_{CM}) = CD44⁺/CD62L⁺, and Naïve T cells (T_N) =
8 CD44⁻/CD62L⁺. Control n=9, HS n=8. Not significant or *p<0.05 by one-tailed, unpaired t-
9 test with/without Welch's correction or Mann-Whitney U test. **F)** Relative mRNA expression
10 levels (in arbitrary units, A.U.) of proinflammatory (G) or anti-inflammatory (H) markers in
11 aortas derived from control animals (grey) or mice subjected to HS (green). qPCR data was
12 normalized to the housekeeping gene GAPDH. Control n=4, HS n=3-4. Analyzed by one-
13 tailed, unpaired t-test with Welch's correction.

14

15 **Figure 4: Transient high salt intake aggravated pro-inflammatory T cell response in**
16 **aortas of AngII-treated ApoE^{-/-} mice: A)** Flow cytometric Zebra plots of CD8⁺ and CD4⁺
17 T cells derived from aortas from ApoE^{-/-} control mice and animals that were transiently
18 treated with high salt via the drinking water (HS). A quantification of the aortic CD4⁺/CD8⁺
19 T cell counts (cells per aorta) is shown on the right side. Control n=10-11, HS n=11. *p<0.05,
20 **p<0.01 by one-tailed Mann-Whitney U test or t-test with Welch's correction. **B/C)** Zebra
21 plots (left) and quantitative analysis of the cell-surface expression of the early activation
22 marker CD69 on aortic CD4⁺/CD8⁺ T cells. Control n=5, HS n=6. Values were analyzed by
23 unpaired, one-tailed t-test with Welch's correction (*p<0.05). **D/E)** Flow cytometric analysis
24 of memory CD4⁺ (D) and CD8⁺ T cells (E) derived from the aortas of ApoE^{-/-} control
25 animals and mice subjected to HS. Upper row: Zebra plots that display the CD44/CD62L

1 expression of CD4⁺ or CD8⁺ T cells. Bottom row: Quantification of the relative amount of
2 memory T cells (% of all CD4⁺/CD8⁺ T cells). Effector memory T cells (T_{EM}) =
3 CD44⁺/CD62L⁻; Central memory T cells (T_{CM}) = CD44⁺/CD62L⁺. Control n=5, HS n=6
4 *p<0.05 or not significant by one-tailed, unpaired t-test with or without Welch's correction.

5

6 **Figure 5: High salt enhanced aortic T cell differentiation and T cell-mediated**
7 **endothelial dysfunction: A)** Relative mRNA expression (in arbitrary units A.U.) of aortic
8 T_H1/T_H17 marker genes after AngII treatment of control and transient HS-treated ApoE^{-/-}
9 mice. qPCR data was normalized to the housekeeping gene GAPDH. Control n=5-6, HS
10 n=8. *p<0.05, **p<0.01, ***p<0.001 by unpaired, one-tailed t-test with Welch's correction
11 or one-tailed Mann-Whitney U test. **B/C)** Intracellular flow cytometry of splenic CD4⁺ (B)
12 and CD8⁺ (C) T cells of AngII-treated control (Control) and transient HS-treated ApoE^{-/-}
13 mice. **B)** Intracellular expression of IL17, IFN γ , TNF α in splenic CD4⁺ T cells. Control n=10,
14 HS n=12. **p<0.01 by one-tailed, unpaired t-test with/without Welch's correction. **C)**
15 Intracellular expression of TNF α or IFN γ in CD8⁺ T cells. Control n=10, HS n=12. Unpaired,
16 one-tailed t-test with Welch's correction or Mann-Whitney U test. **D)** Left: Suppression assay
17 of splenic T_{regs} from transient HS or control mice against experimentally activated
18 CD4⁺CD25⁻ cells from C57BL/6 mice. Control and transient HS n=8. Not significant by one-
19 tailed, unpaired t-test with Welch's correction. Right: Intracellular expression of FoxP3 in
20 splenic CD4⁺ T cells from ApoE^{-/-} mice. Control n=10, HS n=12. Not significant by one-
21 tailed Mann-Whitney U test. **E)** Vessel myography of excised aortas from C57BL/6 mice
22 incubated with supernatants of *in vitro* CD3/CD28 activated CD8⁺ T_C1 cells (left), or CD4⁺ T
23 cells obtained from the spleen of C57BL/6 mice which were further differentiated into T_H17
24 (middle) or T_H1 cells (right). Control n=5, HS n=3. *p<0.05, by 2-way ANOVA.

Fig. 1

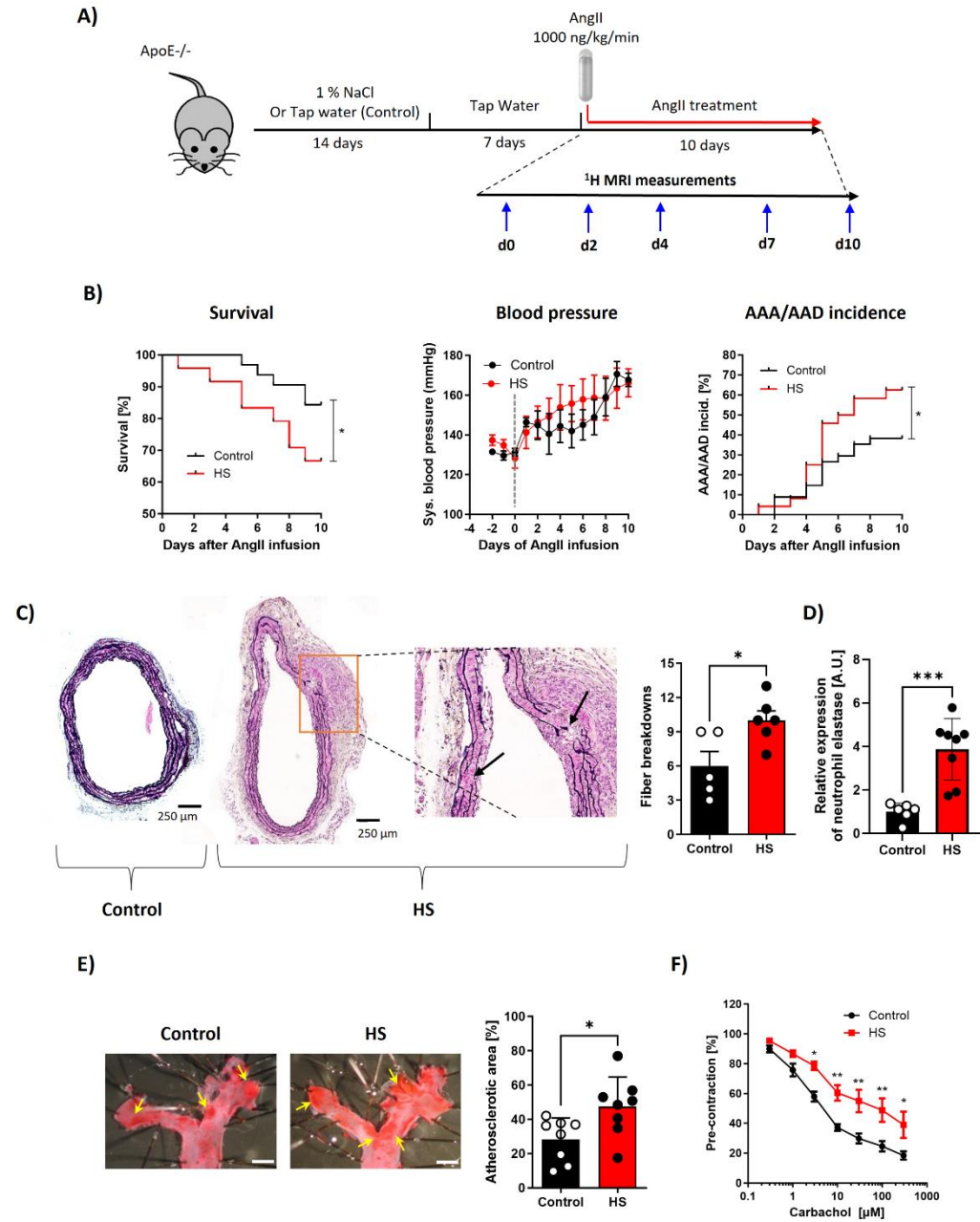


Fig. 2

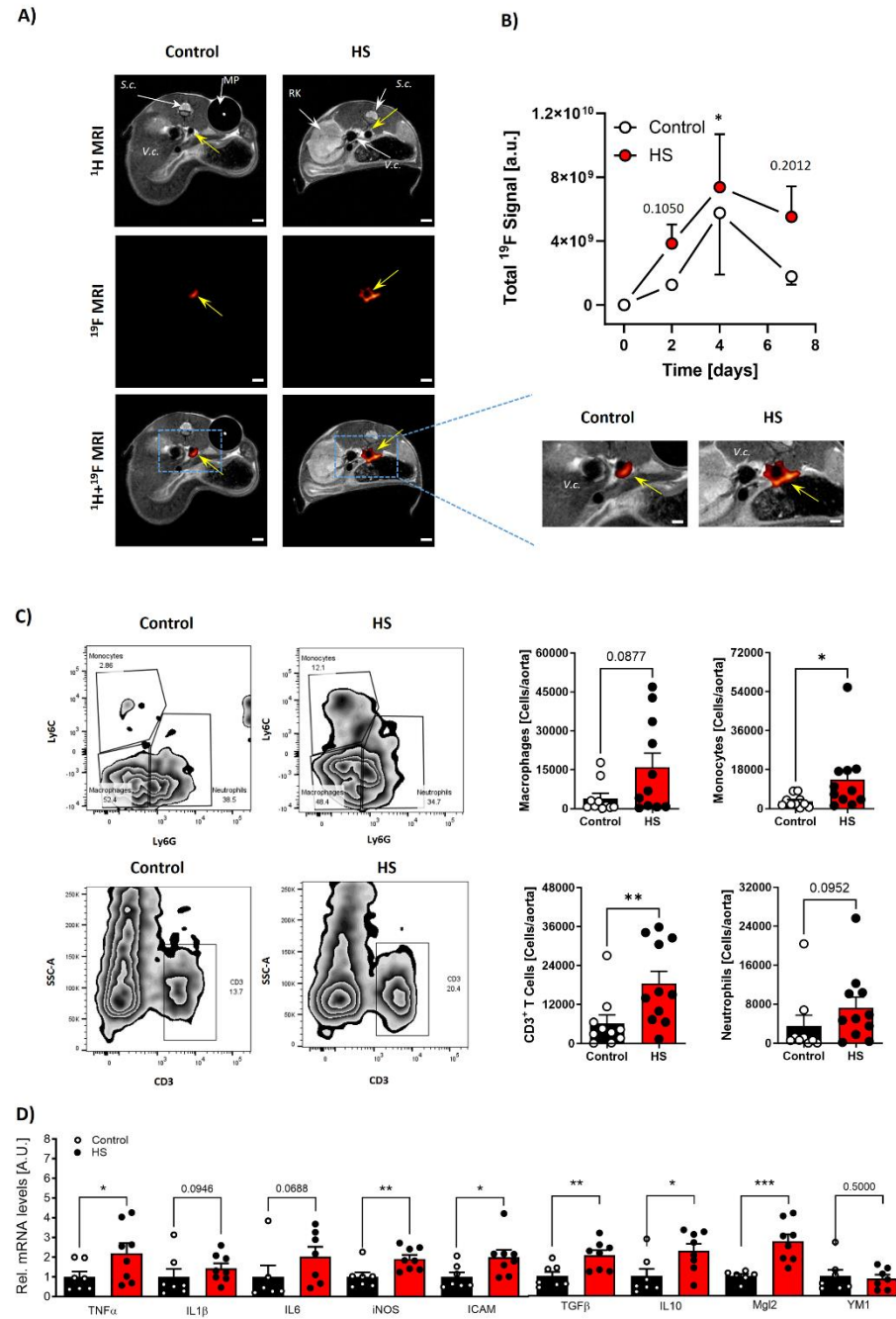


Fig. 3

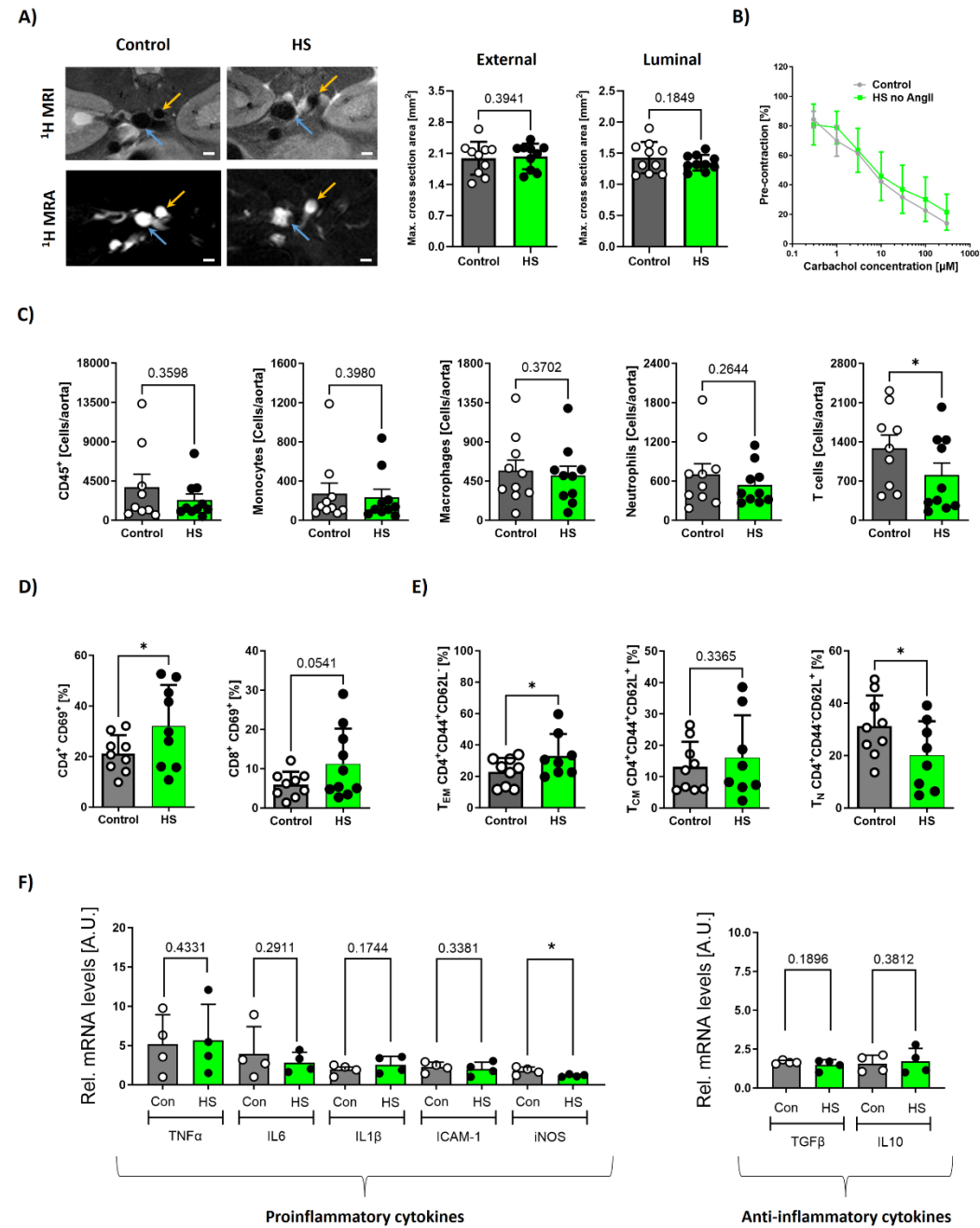


Fig. 4

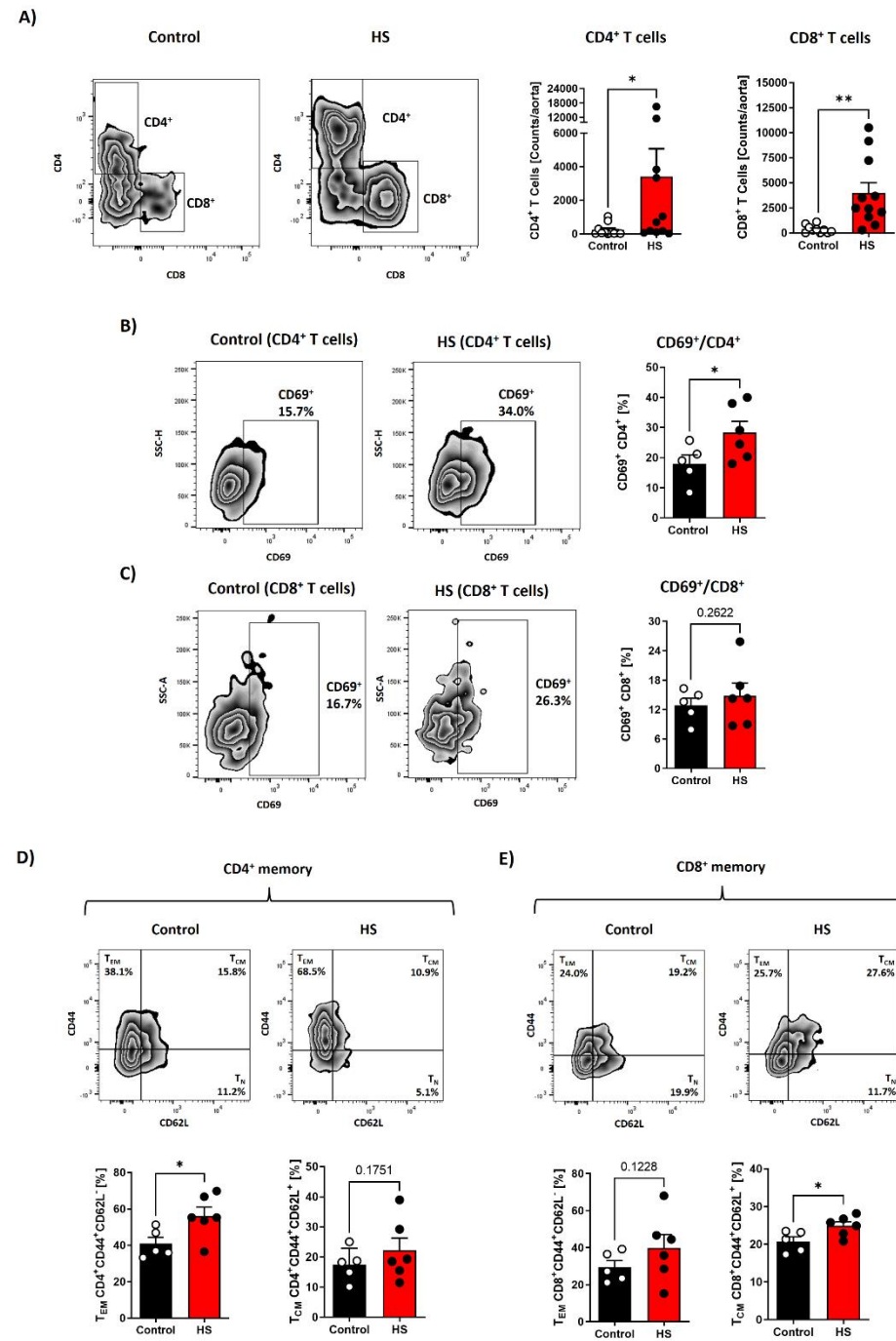
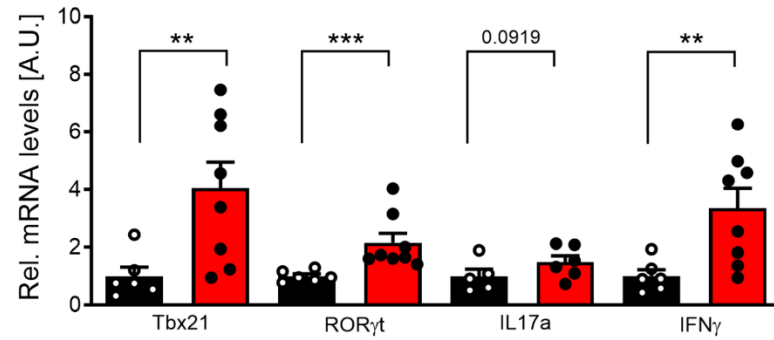
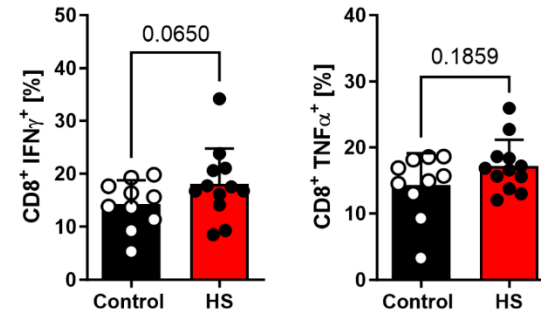


Fig. 5

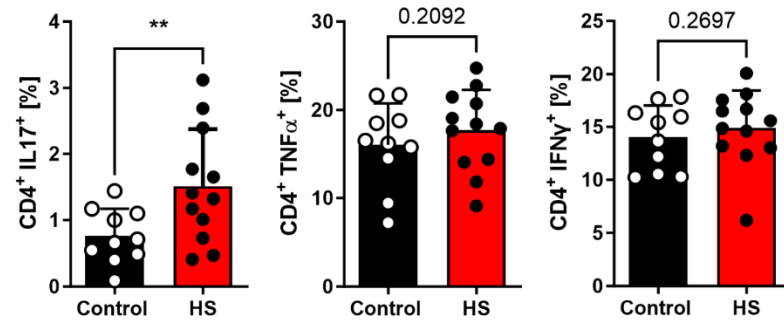
A)



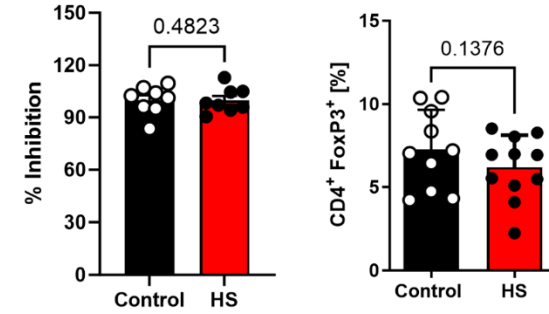
C)



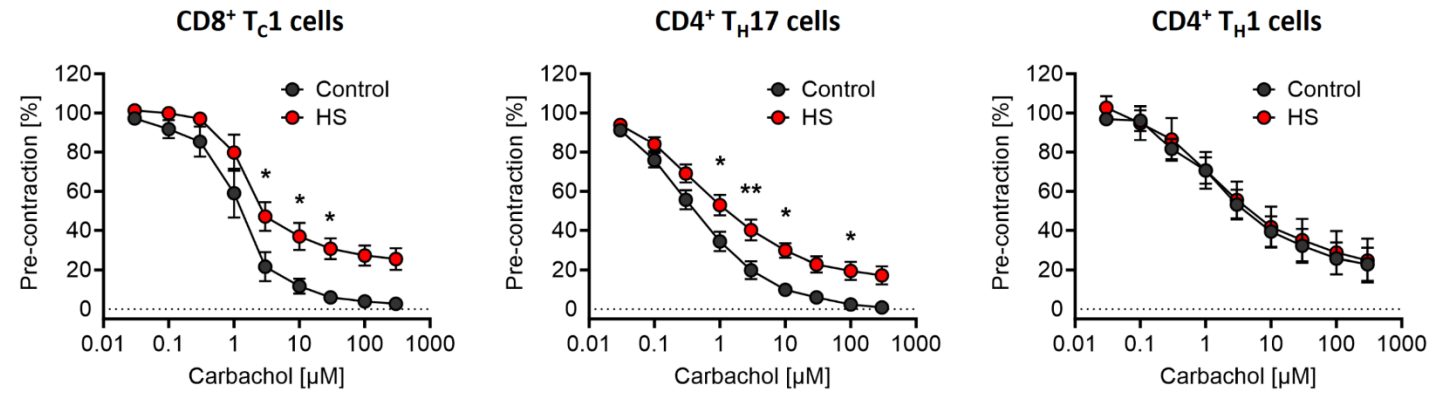
B)



D)



E)



Supplemental Material

Transient high salt intake promotes T cell-mediated hypertensive vascular injury

Short Title: High salt aggravates hypertensive vascular injury

Mina Yakoub¹, Masudur Rahman¹, Patricia Kleimann^{2,3}, Jasmina Hoffe¹, Milena Feige¹, Pascal Bouvain^{2,3}, Christina Alter³, Jennifer-Isabel Kluczny¹⁶, Sophia Reidel⁴, Rianne Nederlof⁴, Lydia Hering¹, Doron Argov¹, Denada Arifaj¹, Marta Kantauskaite¹, Jaroslawnna Meister^{5,6}, Markus Kleinewietfeld^{7,8,9}, Lars Christian Rump^{1,10}, Jonathan Jantsch¹¹, Ulrich Flöge^{12,10}, Dominik N. Müller^{12,13,14,15}, Sebastian Temme^{2,10,16*}, Johannes Stegbauer^{1,10#*}

¹ Department of Nephrology, Faculty of Medicine, University Hospital, Heinrich-Heine-University, Düsseldorf, Germany

² Experimental Cardiovascular Imaging, Department of Molecular Cardiology, Heinrich-Heine-University, Düsseldorf, Germany

³ Department of Molecular Cardiology, Heinrich-Heine-University, Düsseldorf, Germany

⁴ Institut für Herz-Kreislauf-Physiologie, Heinrich-Heine-University, Düsseldorf, Germany

⁵ Institute for Clinical Diabetology, German Diabetes Center, Leibniz Institute for Diabetes Research at Heinrich Heine University, Düsseldorf, Germany;

⁶ German Center for Diabetes Research (DZD e.V.), München-Neuherberg, Germany

⁷ VIB Laboratory of Translational Immunomodulation, VIB Center for Inflammation Research (IRC), Hasselt University, Diepenbeek, Belgium

⁸ Department of Immunology, Biomedical Research Institute, Hasselt University, Diepenbeek, Belgium

⁹ University Multiple Sclerosis Center (UMSC), Hasselt University, Diepenbeek, Belgium

¹⁰ Cardiovascular Research Institute Düsseldorf (CARID), Medical Faculty and University Hospital Düsseldorf, Heinrich-Heine-University, Düsseldorf, Germany

¹¹ Institute for Medical Microbiology, Immunology and Hygiene, Center for Molecular Medicine Cologne (CMMC), University of Cologne, Cologne, Germany

¹² Max Delbrück Center for Molecular Medicine in the Helmholtz Association, Berlin, Germany

¹³ Experimental and Clinical Research Center, a cooperation of Charité-Universitätsmedizin Berlin and Max Delbrück Center for Molecular Medicine, Berlin, Germany

¹⁴ Charité-Universitätsmedizin Berlin, corporate member of Freie Universität Berlin and Humboldt-Universität zu Berlin, Berlin, Germany

¹⁵ DZHK (German Centre for Cardiovascular Research), partner site Berlin, Germany;

¹⁶ Department of Anaesthesiology, Faculty of Medicine, University Hospital, Heinrich-Heine-University, Düsseldorf, Germany

Supplemental Methods

SM1: Transient high salt intake, AngII treatment and blood pressure (BP) measurement

ApoE^{-/-} mice (6 to 10 weeks old) were given 1% salt (NaCl, sodium chloride, VWR chemical, Louvain-la-Neuve, Belgium) in their drinking water for 2 weeks and then switched to normal tap water for 1 week. Subsequently, hypertensive vascular damage was induced by chronic AngII infusion (1000 ng/kg/min) via subcutaneously implanted osmotic minipumps (model 1002, Alzet, Durcet, California, USA). During AngII infusion, MRI scans were performed at different time points. After 10 days of AngII infusion, mice were euthanized for further assessment of inflammatory responses and vascular function. Control mice underwent the same procedures except for pre-treatment with HS (Fig. 1A).

Blood pressure (BP) was monitored using an implantable radiotelemetry device (Data Sciences International, 's-Hertogenbosch, The Netherlands) as described previously¹. Prior to the AngII infusion, the device was implanted under isoflurane anesthesia. The left common carotid artery was dissected and cannulated, and the catheter was carefully placed until the small notch on the tubing was at the vessel opening. The catheter was then secured, and the transmitter was placed subcutaneously. After the procedure, the mice were given seven days to recover. BP and heart rate were continuously measured every 20 minutes at 10-second intervals.

SM2: *In vivo* ¹H/¹⁹F Magnetic Resonance Imaging

Experiments were performed at a vertical 9.4 T Bruker AVANCEIII Wide Bore NMR spectrometer (Bruker) operating at frequencies of 400.21 MHz for ¹H and 376.54 MHz for ¹⁹F measurements using microimaging units as described previously². Mice were anesthetized with 1.5% isoflurane and were kept at 37°C during the measurements. For gated magnetic resonance imaging (MRI) acquisitions, respiration was monitored by means of a pneumatic pillow positioned at the animal's back. Vital functions were acquired by an M1025 system (SA

Instruments) and used to synchronize data acquisition with respiratory motion. Data were acquired using a 25-mm quadrature resonator tuneable to ^1H and ^{19}F . To visualize the anatomy of the region of interest, ^1H MR reference images from the abdomen were acquired using a rapid acquisition and relaxation enhancement sequence [RARE; field of view (FOV) = $2.56 \times 2.56 \text{ cm}^2$, matrix = 256×256 , $0.1 \times 0.1 \text{ mm}^2$ in plane resolution, 1 mm slice thickness (ST); repetition time (TR) = 2500 ms; RARE factor = 16, 6 averages (NA), acquisition time (TAcq) = $\sim 5 \text{ min}$]. ^1H MR time-of-flight angiography to visualize dilatation or narrowing of the aorta via its blood flow pattern was carried out by a ^1H fast low angle shot (FLASH) 2D flow compensated sequence; FOV = $2.56 \times 2.56 \text{ cm}^2$, matrix = 256×256 , $0.1 \times 0.1 \text{ mm}^2$ in plane resolution, ST = 0.5 mm; 0.25 mm overlap, 100 slices; TR = 10 ms; NA = 6; TAcq = 4 min). After the acquisition of the morphological ^1H images, the resonator was tuned to ^{19}F and anatomically matching ^{19}F datasets were recorded. The reference power and the receiver gain were kept constant between the measurements to verify the comparability of the ^{19}F measurements. Anatomically matching ^{19}F images were recorded from the same FOV with a ^{19}F RARE sequence (matrix = 64×64 , $0.4 \times 0.4 \text{ mm}^2$ in plane resolution, ST = 1 mm, TR = 4,000 ms, RARE factor = 32, NA = 25, and TAcq = 34 min).

To visualize early infiltration of phagocytic immune cells like monocytes, perfluorocarbon nanoemulsions (PFCs) were applied intravenously 2h post minipump implantation, on day 2 and day 4. Combined $^1\text{H}/^{19}\text{F}$ MRI measurements were conducted 24-48 h post PFC injection to verify the infiltration of PFC-labelled phagocytic cells¹. Details about MRI data analysis and preparation and characterization of PFCs are found in the supplement (SM3 and SM4).

SM3 MRI Data Analysis

To quantify the luminal or the external diameter of the aorta, the cross-section either of the flowing blood (luminal diameter) or of the aortic wall based on the anatomical scans was

determined in Fiji using the Bruker Plugin. Since the aortic wall is only 100 μm in diameter, which is hardly detectable by conventional ^1H MRI, we determined the extension of the external diameter. The ^{19}F MR data was quantified using Fiji and appropriate Bruker plugins. To this end, ROIs (regions of interest) were drawn around the ^{19}F signal to determine both the mean and total ^{19}F intensity. Background ROIs were placed outside the animals. The SNR was calculated by: ^{19}F SNR = (^{19}F signal intensity – mean background signal) / standard deviation of the background signal (noise). The total amount of the aortic ^{19}F signal was determined by summarizing the ^{19}F intensities of all the aortic ROIs.

SM4: Preparation and Characterization of Perfluorocarbon Nanoemulsions (PFCs)

Perfluorocarbon nanoemulsions (PFCs) were prepared as described previously¹. Lipids (E80S, 35 mM) (Lipoid GmbH) were dissolved in phosphate glycerol buffer, perfluoro-15-crown-5 ether was added, and the mixture was processed by high-shear mixing (Ultraturrax) to generate a pre-emulsion. The pre-emulsion was then subjected to microfluidization (M110P, Microfluidics) for five cycles at 1,000 bar. PFCs were transferred to glass vials and sterilized by autoclaving at 121°C, 1 bar for 20 min, and subsequently analyzed by dynamic light scattering for quality control (see below).

Dynamic Light Scattering: The mean intensity-weighted hydrodynamic diameter was determined. The PFCs were diluted 1:100 (v/v) with MilliQ water. Data acquisition was performed on a Nanotrak Wave II (Microtrac MRB) at 25 °C and the following parameters were determined as described previously²: Particle size as averaged hydrodynamic diameter (d_z , mean intensity-weighted); width of the particle size distribution as polydispersity index (PDI) and zeta (ζ) potential in mV. Size and PDI were determined in five measurements each consisting of five sub-runs, measurements of the ζ potential were performed with the same sample thereafter.

SM5 Oil Red O staining (ORO) to assess atherosclerotic plaques

Aortic arches were dissected and incubated in 4 % PFA at 4°C overnight. After the removal of adventitia, aortic arches were stained with Oil red O solution (Oil Red O, Sigma-Aldrich Chemie GmbH) as described previously¹. In brief, the Oil red O (ORO) solution (0.4 g ORO powder dissolved in 80 ml methanol) was freshly prepared by mixing with 1 M sodium hydroxide (JT Baker, ThermoFisher) in a ratio of 2:7. Aortas were incubated in 78 % methanol for 5 minutes, then in ORO staining solution for 90 minutes, and finally in 78 % methanol for 10 minutes. Quantification of atherosclerosis was determined as the percentage of the area of the red-stained plaques from the total area of the aortic arch using ImageJ software.

SM6: Movat staining (Elastic fiber breaks)

To evaluate the breakdown of elastic fibers in the aorta, Movat staining was utilized¹. This involved fixing the slides in Bouin's solution at 50°C for 10 minutes, followed by exposure to 5% sodium thiosulfate for 5 minutes, 1% alcian blue for 15 minutes, and alkaline alcohol for 10 minutes at 60°C. We then prepared a Movat Weigert's solution by combining 2% alcohol hematoxylin, ferric chloride stock solution, and iodine stock solution in a 3:2:1 ratio, and stained the tissues in this solution for 20 minutes. Next, we used a crocein scarlet acid/fuchsin working solution (in a 3:1 ratio) to stain the slides for 2 minutes. The slides were then treated with 5% phosphotungstic acid for 5 minutes and immediately transferred to 1% acetic acid for 5 minutes, with washing between each step. Finally, the slides were dehydrated in 95% ethanol, followed by two 1-minute treatments with 100% ethanol, and then two 5-minute treatments with xylol. The tissues were mounted in Roti-Mount HP68.1 mounting medium and covered. We manually counted aortic fiber breakdown in three consecutive slides and calculated an average for each mouse. All chemicals were purchased from Sigma, Chempur, Microm, and Carl-Roth.

SM7: Quantitative real-time PCR

The abdominal or thoracic aorta, along with the PVAT, were dissected. The aortas were then further processed according to the manufacturer's protocol. Aortas were transferred to RLT solution with 10% β -mercaptoethanol, ruptured to destroy the tissue, and centrifuged to remove genomic DNA (gDNA), carbohydrates, protein, and other impurities¹. DNase enzyme was used to ensure that all DNA impurities were removed. The isolated mRNA was then collected in 50 μ l of RNase-free water and its amount was quantified spectrophotometrically. The QuantiTect® (Qiagen) Reverse Transcription kit was used to obtain complementary DNA (cDNA). For the subsequent RT-qPCR GAPDH primer was used as a housekeeping control. A master mix including 10 μ L/well sybr green, 0.1 μ L/well forward and 0.1 μ L/well reverse primers, and 8.8 μ L/well RNase free water was used for qPCR. The master mix was pipetted into a 96-well plate, followed by 1 μ L/well cDNA. The plate was sealed and RT-qPCR was run with the 7300 Real-time PCR system (ThermoFisher, Waltham, USA). mRNA quantification was based on the fluorescence threshold. For a list of qPCR primers, please refer to the supplementary table (Table S3).

SM8: Isolation, activation, and differentiation of splenic T cells

Spleens from C57BL/6 were carefully excised, washed in phosphate buffer, and then passed through a 100 μ m mesh to generate a single-cell solution¹. The cells were then centrifuged (300 \times g, 10 min, 4 °C), washed twice with MACS buffer, and finally resuspended in 500 μ l of MACS buffer. Splenocytes were then passed through a 30 μ m mesh to remove cell aggregates. Naïve CD4⁺ or CD8⁺ T cells were then isolated by magnetic bead separation (naïve CD4 or naïve CD8 T cell Isolation mouse Kit™, Miltenyi Biotec or Easy Sep Isolation Kit, Stem-cell technologies) according to the producer's protocol. Isolated cells were then resuspended in

RPMI 1640 medium that was supplemented by 10% FCS, 1% Penicillin/Streptomycin solution, 1% L-Glutamine (Sigma), 1% Non-essential amino acids (NEAA)(Sigma), 1% sodium pyruvate (Sigma) and 50 μ M β -Mercaptoethanol (Gibco). Cell counts were determined using a Neubauer counting chamber.

To stimulate T-cells we used CD3/CD28 antibodies. First, anti-CD3 (2 μ g/ml in 50 μ l PBS) was coated on the bottom of a flat bottom 96-well plate at 37 °C for 60 min. Then, 100 000 T cells resuspended in 50 μ l medium and 50 μ l of anti-CD28 antibody (8 μ g/ml) in the medium were added per well. Finally, the volume was adjusted to 200 μ l of medium added per well and cells were cultivated for 72 h. For high salt, the NaCl concentration was adjusted to 180 mM (140 mM NaCl = control condition). For the assessment of the percentage of naïve T cells that underwent activation into effector cells, cytokines measurement was done on the supernatant using Quantikine ELISA kits (R&D systems, USA).

In some experiments, CD4⁺ T cells were activated by aCD3/aCD28 and then further differentiated into T_{H1} or T_{H17} direction as described previously³. In Brief, for differentiation, CD4⁺ T cells were stimulated with IL-12 (20 ng/ml, BioLegend) and anti-IL-4 (10 μ g/ml, Clone 11B11, BioLegend) mAb for T_{H1} or with TGF β 1 (2 ng/ml, R&D Systems) and IL-6 (40 ng/ml, R&D Systems) for T_{H17} differentiation. Afterwards, the supernatant was collected for vascular function experiments.

SM9: Impact of T cell supernatant on aortic relaxation

Thoracic aortic rings of wild-type mice were incubated in 100 μ l of T cell supernatant (see SM8) and 100 μ l Williams E medium supplemented with 2 mM L-glutamine (Sigma-Aldrich GmbH), 100 g/L glucose (Carl Roth GmbH, Karlsruhe, Germany) and 10 μ g/ml ciprofloxacin (Sigma-Aldrich GmbH) at 37°C in an oxygenated atmosphere with 5% CO₂ for 22 hours. To exclude the direct effects of NaCl on vascular function, NaCl concentrations in the incubation

buffer were equalized. After incubation, the aortic rings were placed in Krebs Henseleit solution with the ionic composition of 118 mM NaCl, 4.7 mM KCl, 2.5 mM CaCl₂, 1.03 mM KH₂PO₄, 0.45 mM MgSO₄, 11.1 mM of glucose and 25 mM NaHCO₃ and mounted in a wire myograph (Multi Myograph Model 610 M, Danish Myo Technology, Denmark). The solution was gassed continuously with carbogen, and the temperature was maintained at 37°C. 5 mN resting tension was applied to the aortic rings followed by 30-40 minutes of equilibration in the presence of diclofenac (3 μM) (Sigma-Aldrich GmbH). Endothelial-dependent vasorelaxation was assessed in norepinephrine (1 μM) induced precontracted aortic rings by cumulative application of carbachol (0.03 μM-300 μM).

SM10: Assessment of T_{reg} cell function

Splenic T cells were isolated from C57BL/6 mice as described above and regulatory T cells were obtained from spleens of transient HS-treated animals using magnetic bead separation (CD4⁺CD25⁺ regulatory T cell isolation kit, Miltenyi Biotec). T cells were labelled with CFSE (ThermoFisher) and 100 000 CFSE-stained responder T cells were incubated with 100.000 T_{reg} cells from THS-treated mice (or corresponding T_{reg} cells from sham-treated animals) in the presence of 100.000 irradiated CD4-depleted splenocytes from naïve C57BL/6 mice. Cells were activated by 2 μg/ml anti-CD3 and CD28 for 72h. Subsequently, cells were analyzed by flow cytometry and the number of cell divisions was determined by calculating the mean fluorescence intensity of the CFSE signal.

SM11: In vitro experiments with neutrophil granulocytes

Isolation of neutrophils: For isolation of neutrophils from the bone marrow (femur, tibia), mice were sacrificed via cervical dislocation and bones were dissected. Afterwards, bone

marrow was isolated via a centrifugation-dependent protocol and neutrophils were isolated via an isolation kit (EasySep™ mouse neutrophil enrichment kit, STEMCELL Technologies).

HS and migration: 1×10^5 neutrophils were transferred in a ThinCert insert (3 μm pore) (Greiner Bio-One GmbH) in 200 μl RPMI while the lower chamber was filled with 750 μl RPMI with 0.1 μM fMLP (Sigma-Aldrich) as chemoattractant. For HS, an additional 40 mM NaCl was added to the medium. The migration assay was stopped after 1 hr at 37°C. The lower part was transferred into FACS tubes, centrifuged at 300xg for 5 min, and cells stained against CD45, CD11b and Ly6G to identify and count the migrated neutrophils via flow cytometry. Dead cells were excluded from the analysis by DAPI staining.

Migration assay - Coculture with T cells: 1×10^5 neutrophils were co-cultivated with 1×10^5 T cells (CD4⁺ or CD8⁺ T cells isolated from the spleen of male C57BL/6 (10-12 weeks of age)) for 1 hr in 200 μl RPMI. Afterwards, cells were transferred in a ThinCert insert (3 μm pore) (Greiner Bio-One GmbH) in 200 μl RPMI while the lower chamber was filled with 750 μl RPMI with 0.1 μM fMLP (Sigma-Aldrich) as chemoattractant. The migration assay was stopped after 1 hr at 37°C and cells were analyzed as described above.

Migration assay - Impact of IFN γ and IL17: First experiment: 1×10^5 neutrophils were stained against Ly6G for 20 min at 4°C and then transferred in a ThinCert insert (3 μm pore) in 200 μl DMEM+FCS [10 %], while the lower chamber was filled with 1 ml DMEM+FCS with 0.1 μM fMLP, 5 ng/ml IFN γ (Sigma-Aldrich), 25 ng/ml IL17 (BioLegend) or a combination of these molecules as chemoattractants. As a control, no chemokine/cytokine was added to the lower chamber. Second experiment/Prestimulation of neutrophils: 1×10^6 neutrophils were stained against Ly6G for 20 min at 4°C and then transferred in 1.5 ml reaction tubes filled with 1 ml DMEM+FCS containing 5 ng/ml IFN γ , 25 ng/ml IL17 or IFN γ + IL17 for prestimulation. As a control, no chemokine/cytokine was added to the reaction tube. Incubation was stopped after 1 hr at 37°C. 1×10^5 neutrophils were counted by flow cytometry

and transferred in a ThinCert insert in 200 μ l DMEM+FCS, while the lower chamber was filled with DMEM+FCS with 0.1 μ M fMLP as chemoattractant. For both settings, the migration assay was stopped after 2 hr at 37°C. The lower part was transferred into FACS tubes, centrifuged at 300xg for 5 min, and migrated neutrophils were counted via flow cytometry. Dead cells were excluded from the analysis by DAPI [1 μ g/ml] staining.

Neutrophil extracellular trap (NET) formation: T cells were isolated by MACS from the spleen of male mice activated with anti-CD3/anti-CD28 for 72 h in a medium with normal salt or an additional 40 mM salt. Then, 150 000 bone marrow-derived neutrophils (in 100 μ l medium without FCS) and 150 000 CD3/CD28 activated T cells (in 150 μ l medium with 10 % FCS) were seeded per well in a 96-well plate. Cells were incubated for 4 hours at 37 °C. Then, 50 μ l Quant-iT™ PicoGreen®dsDNA reagent (Thermo Fisher Scientific (P7581)) in a dilution of 1:100 was added to each well and incubated for 10 minutes at 37 °C. After incubation, fluorescence was measured using a fluorescence microplate reader and standard fluorescein wavelengths (excitation ~480 nm, emission ~520 nm).

SM12: Flow cytometric analysis of immune cell subtypes

Flow cytometric analysis of the aorta was performed on mice immediately after sacrificing them. The abdominal aorta, along with the perivascular adipose tissue, was carefully dissected from the diaphragm to the bifurcation of the aorta. To obtain a single-cell suspension, the aorta was digested with a collagenase-containing solution (600 U/ml Collagenase type II and 60 U/ml DNase I in HBSS, for 30 min, 37 °C). The cells were then washed twice and stained with antibodies against CD45, F4/80, CD3, CD4, CD8 α , CD44, CD62L, CD69, CD11b, Ly6G, and Ly6C. We used fluorescence minus one (FMO) controls in each staining panel to set thresholds and gates to precisely identify immune cell types and the activation/memory status of the cells.

The gating scheme for immune cells isolated from the aorta is shown in the supplement (Fig. S4 and S5).

To analyze T cell subsets in the spleen, the spleens were fragmented into small pieces and passed through a 100 μ m filter. The cells were restimulated for 4 hours using RPMI 1640 medium (Sigma-Aldrich) containing 10% FCS, 1% Penicillin/Streptomycin solution (Biochrome), 50 ng/mL PMA (Phorbol-12-Myristat-13-Acetat; Sigma-Aldrich), 750 ng/mL Ionomycin (Sigma-Aldrich), and 0.75 μ g/mL Monesin (GolgiStop Protein transport inhibitor, BD Bioscience). After incubation, cells were washed twice with 200 μ L FACS buffer, and LIVE/DEAD® Fixable Aqua (405 nm) Stain (Invitrogen™ Life Technologies) was added to exclude dead cells. Cells were permeabilized and fixed using Foxp3/Transcription Factor Fixation/Permeabilization kit (eBioscience), followed by staining with antibodies against CD3, CD4, CD8, IL-17, IFN γ , TNF α , and Foxp3 for 30 min at 4 °C in the dark.

ApoE^{-/-} mice were treated with 1% NaCl via the drinking water for two weeks and finally sacrificed by cervical dislocation. After harvesting the mesenteric lymph nodes, the excess fat was removed and the lymph nodes were squeezed through a 100 μ m sieve using a syringe plunger (1mL)¹. The lymph nodes were kept moist with working buffer (0.5% HAS (human serum albumin), Albutein 50g/l 12,5g/250ml, Grifols in PBS (1x) self-made). The cell suspension was then centrifuged at room temperature and 300g for 5 minutes. Immediately after sample processing, the pellet was resuspended in a 500 μ l working buffer. For antibody staining, 100 μ l of the cell solution was pipetted into a FACS tube (#55.1579.002, 5ml Tube 75x12mm, Sarstedt), and a distinct number of CountBright™ Absolute Counting Beads (#C36950 Lot.: 2628756, Thermo Fisher Scientific) (0,47x10⁶ Beads/50 μ l Sample) was added to each tube to determine absolute numbers of cells. Cells and Beads were centrifuged at room temperature and 300g for 5 min, and the supernatant was discarded. To prevent unspecific

binding, the cells were treated with TruStain FcXTM (anti-mouse CD16/32) (#101320, BioLegend) and additionally stained with the ViaKrome 808 Fixable Viability Dye (#C36628, Beckman Coulter) for 20 minutes at room temperature protected from light, followed by centrifugation for 5 minutes at 300g and room temperature, supernatant was discarded. Staining solution was added, including CD3 (#363-0032-80, Thermo Fisher), CD45 (#364-0451-80, Thermo Fisher), CD19 (#376-0193-80, Thermo Fisher), CD11c (#404-0114-82, Invitrogen), CD25 (#102042, BioLegend), CD69 (#104529, BioLegend), F4/80 (#123149, BioLegend), CD8 (#100750, BioLegend), CD44 (#553133, BD Bioscience), Ly6G (#127616, BioLegend), CCR2/CD192 (#150636, BioLegend), NK1.1 (#108714, BioLegend), Ly6C (#128007, BioLegend), CD62L (#104410, BioLegend), CD11b (#101226, BioLegend), Siglec-F (#155508, BioLegend), CD4 (#100536, BioLegend). Cells were resuspended and stained for 20 min at RT in the dark, followed by centrifugation for 5 minutes at 300g and RT. The supernatant was removed, and the cell pellet was resuspended in 200 µl working buffer. The tubes were stored at 4 °C until measurements. Flow cytometric data were acquired using a CytoFLEX LX flow cytometer (Beckman Coulter) and analyzed using Kaluza Software (Beckman Coulter).

Supplemental References

1. Bartolomaeus H, Balogh A, Yakoub M, Homann S, Markó L, Höges S, Tsvetkov D, Krannich A, Wundersitz S, Avery EG, et al. Short-Chain Fatty Acid Propionate Protects From Hypertensive Cardiovascular Damage. *Circulation*. 2019;139:1407–1421.
2. Temme S, Yakoub M, Bouvain P, Yang G, Schrader J, Stegbauer J, Flögel U. Beyond Vessel Diameters: Non-invasive Monitoring of Flow Patterns and Immune Cell Recruitment in Murine Abdominal Aortic Disorders by Multiparametric MRI. *Frontiers in Cardiovascular Medicine*. 2021;8:1421.
3. Kleinewietfeld M, Manzel A, Titze J, Kvakan H, Yosef N, Linker RA, Muller DN, Hafler DA. Sodium chloride drives autoimmune disease by the induction of pathogenic TH17 cells. *Nature*. 2013;496:518–522.

Supplemental Tables

Table S1: The ARRIVE guidelines 2.0: author checklist

Item/Criteria:	Fulfilment place or reason
Study design	The study involved using mice that lacked the apolipoprotein E gene. These mice were given 1% salt water to drink for two weeks, while another group of mice were given tap water. After two weeks, all the mice were returned to drinking tap water for one week. Then, a group of mice were given osmotic minipumps containing Angiotensin II, while the control group received no treatment. The pumps were implanted under the skin and the treatment lasted for 10 days.
Sample size	In each experiment, the exact number of mice used is mentioned in the legend of each figure.
Inclusion and exclusion criteria	Inclusion criteria were 8 to 12-week-old male ApoE ^{-/-} mice, as mentioned in section 2.1. Monitoring of health assessment was carried out on the mice such as routine free from infection tests. In case mice reached an endpoint described in the animal protocol (for example weight loss more than defined) the mice were sacrificed.
Randomisation	In case of variances (such as age) within a batch of mice, the mice were randomized equally over each experimental group.
Blinding	The researcher who performed the read-out assessments was blinded to the assignment of the mouse subjects to the experimental groups.
Outcome measures	Several outcomes were measured such as the overall survival of the mice, degree of atherosclerosis, in vivo noninvasive measurement (e.g.: MRI for AAA/AADs) and ex vivo terminal measurements (e.g.: Aorta and spleen flow cytometry). The detailed outcome measurement is mentioned in each figure.
Statistical methods	Mentioned in section 2.4
Experimental animals	ApoE ^{-/-} mice that were backcrossed on a C57BL/6 background for at least 10 generations, males, 8-12 weeks. Mice were obtained from external vendors and genotyped in-house
Experimental procedures	Experimental procedures are illustrated in figure 1A
Results	A descriptive summary, n number of replicates, statistical method, and SEM are mentioned below each figure

Table S2: Antibodies used for flow cytometry

All antibodies are targeted against the murine versions of the indicated antigens and were purchased from Biolegend (San Diego, USA), eBioscience (San Diego, USA), Miltenyi Biotec (Bergisch Gladbach, Germany), and BD Pharmingen (Franklin Lakes, NJ, USA). A list of all the antibodies used is provided in the table below (Supplementary table S2).

Antigen/Fluorochrome	Manufacturer	Catalogue number	Antibody Clone
FCR blocking reagent	Miltenyi	130-092-575	
Ly6G-FITC	BD Pharmingen	551460	1A8
Ly6C-APC/Fire750	Biolegend	128046	HK1.4
CD45-APC	BD Pharmingen	559864	30-F11
CD11b-PE/Cy7	eBioscience	25-0112-82	M1/70
CD4-PerCP/Cy5.5	BD Pharmingen	550954	RM4-5
CD44-AlexaFluor488	Biolegend	103015	IM7
CD69-FITC	eBioscience	11-0691-82	H1.2F3
CD62L-BV510	Biolegend	104441	MEL-14
CD8-APC/Fire750	Biolegend	100765	53-6.7
CD45-PE/Cy7	BD Pharmingen	552848	30-F11
CD3-FITC	Miltenyi	130-119-798	REA641
CD8-APC/Vio770	Miltenyi	130-120-806	REA601
IL17-PE	Miltenyi	130-112-009	REA660
IFN γ -PE.Cy7	Miltenyi	130-117-502	REA638
TNF α -APC	Miltenyi	130-123-277	REA636
Foxp3-PerCP/Cy5.5	Miltenyi	130-111-681	REA788
CD3-BUV395	ThermoFisher	363-0032-80	17A2
CD45- BUV496	ThermoFisher	364-0451-80	30-F11
CD19- BUV661	ThermoFisher	376-0193-80	1D3
CD11c-BUV421	Invitrogen	404-0114-82	N418
CD25-BV510	BioLegend	102042	PC61
CD69-BV605	BioLegend	104529	H1.2F3
F4/80-BV650	BioLegend	123149	BM8

CD8a-BV785	BioLegend	100750	53-6.7
CD44-FITC	BD Pharmingen	553133	IM7
Ly6G-PerCP.Cy5.5	BioLegend	127616	1A8
CD192(CCR2)- PE.Dazzle594	BioLegend	150636	SA203G11
NK1.1-PE.Cy7	BioLegend	108714	PK136
Ly6C-PE	BioLegend	128007	HK1.4
CD62L-PE.Cy5	BioLegend	104410	MEL-14
CD11b-APC.Cy7	BioLegend	101226	M1/70
CD170(SiglecF)-APC	BioLegend	155508	S17007L
CD4-Alexa700	BioLegend	100536	RM4-5

Table S3: Sequence of DNA-primers for qPCR:

GAPDH: Forward:GTGTTCCCTACCCCAATGTGT Reverse: GTCCTCAGTGTAGCCCAAGATG
TNFα: Forward: ATGTCTCAGCCTCTTCTCATTC Reverse: GTCTGGGCCATAGAACTGATGA
TGFβ: Forward: GCTGCGCTTGCAGAGATTA AAA Reverse: CGTCAA AAGACAGCCACTCA
IL-6: Forward: CAGAGGATACCACTCCCAACA Reverse: GCCATTGCACA ACTCTTTTCTC
IL17a: Forward: GGCCCTCAGACTACCTCAACC Reverse: TGAGCTTCCCAGATCACAGAG
IL1β: Forward: GGATGAGGACATGAGCACCTT Reverse: CTAATGGGAACGTCACACACC

IFN γ , iNOS, Tbx21, RoR γ t, Il10, Mgl2, ICAM, and YM1 primers were purchased as Taqman sequences (Thermo Fischer Scientific, Massachusetts, USA) with a proprietary sequence.

Supplemental Figures

Figure S1

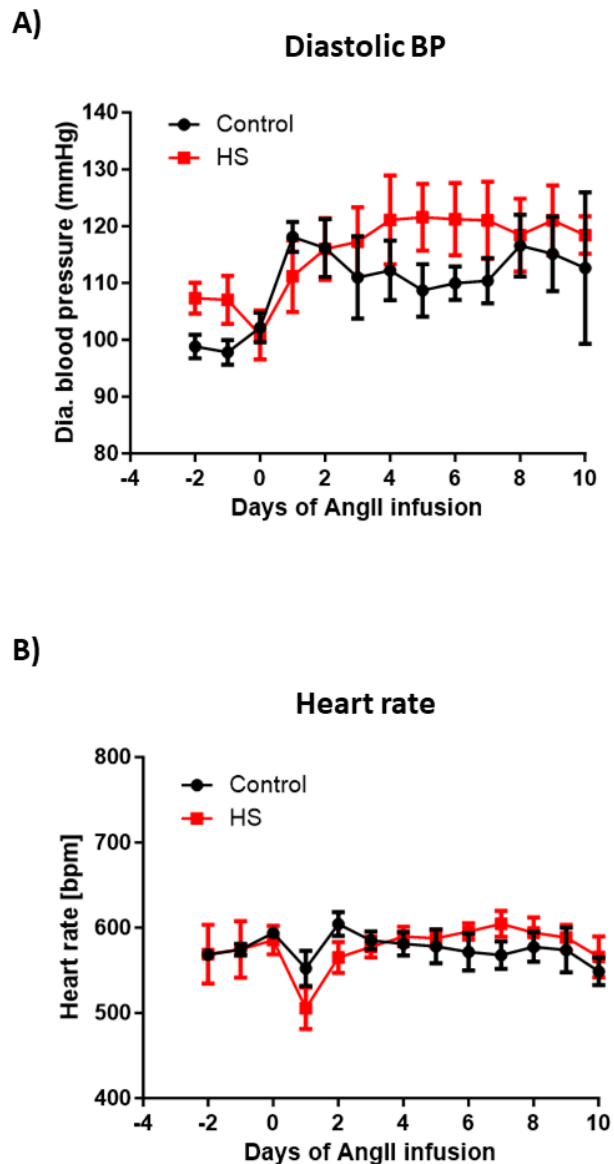
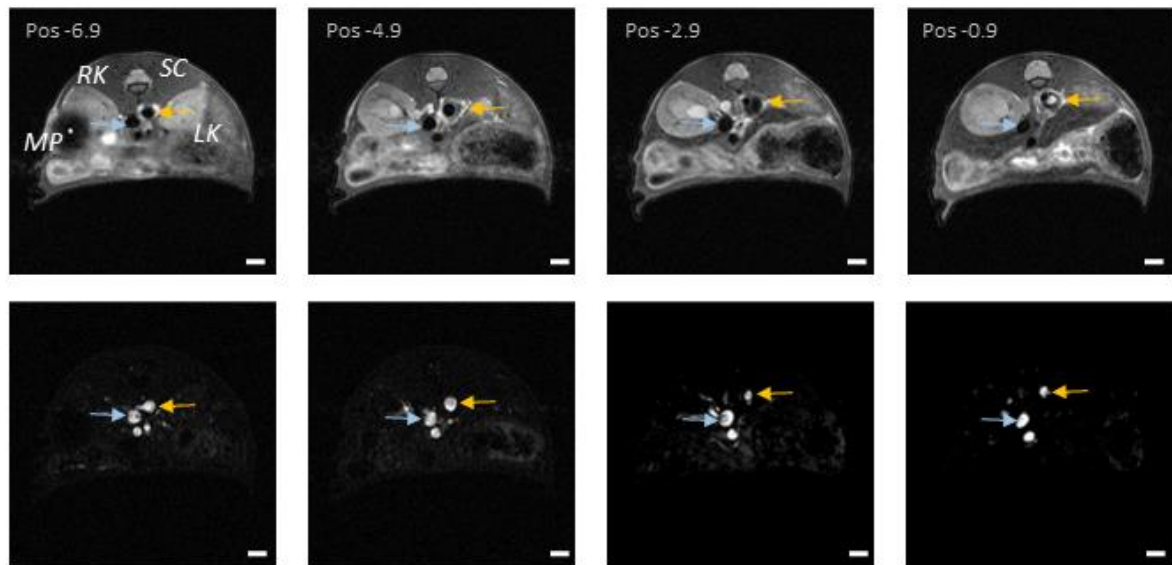


Figure S1: Blood pressure and heart rate: A) Radiotelemetric measurements of diastolic blood pressure B) Heart rate measurements in mice before and after implantation of angiotensin II minipumps. Red: Before implantation of osmotic minipumps, mice were transiently treated with 1% NaCl in the drinking water for 14 days, followed by a period of one week with normal tap water (HS). Black: Controls with normal tap water over the whole period of the experiment. Control n=5, HS n=5. Not significant, by 2-way ANOVA.

Figure S2

A) Aortic Dissection



B) Aortic Aneurysm

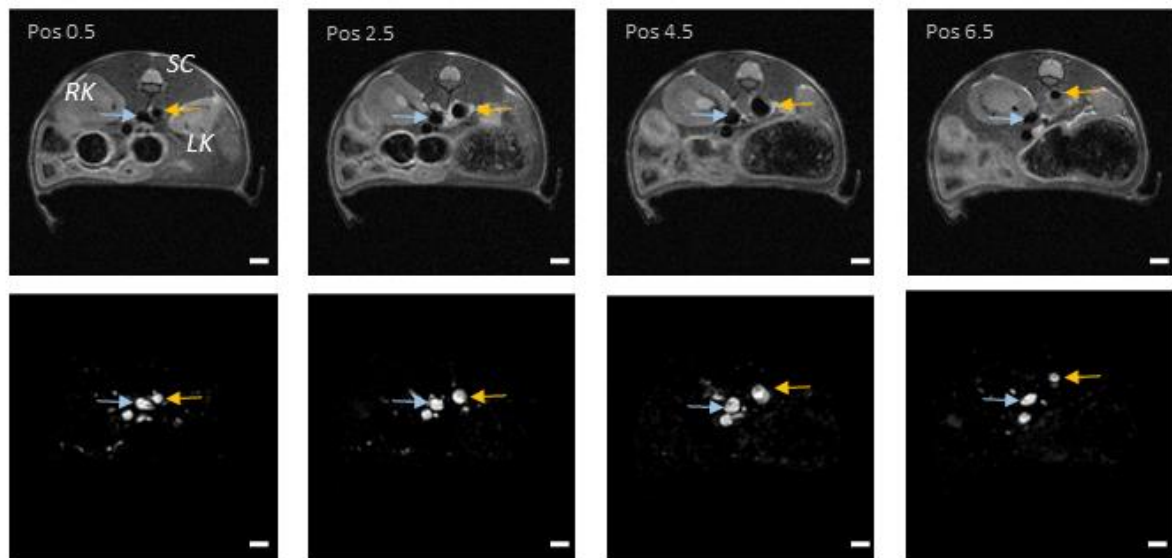


Figure S2: MRI of aortic dissections and aneurysms: A/B) Anatomical (upper lane) and angiographic (lower lane) axial ^1H MRI images from caudal to cranial direction to visualize the appearance of abdominal aortic dissections (A) or aneurysms (B). Yellow arrow = aorta, Blue arrow = *vena cava inferior*. RK = right kidney, LK = left kidney, SC = spinal cord, MP =

osmotic minipump. Numbers in the upper part of the anatomical images represent the relative position of the slices in the Z-direction (cranial → caudal). Scale bars = 1 mm.

Figure S3

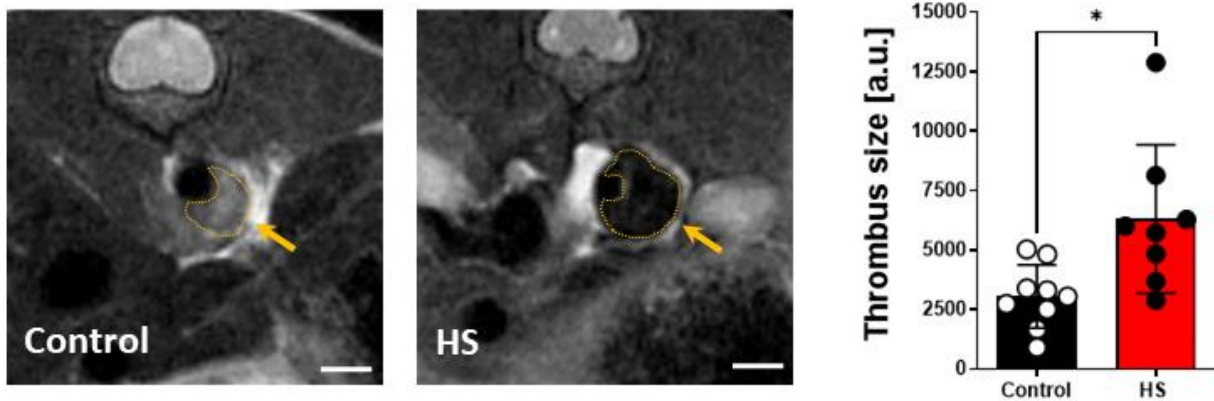


Figure S3: MRI of thrombus formation in aortic dissections: A) Anatomical ¹H MRI images of aortic dissections from control and HS mice. The highlighted area represents the area of the thrombi. **B)** Quantification of the area of the thrombi (arbitrary units = a.u.). Control n=10, HS n=8.*p<0.05, by one-tailed t-test with Welch's correction. Scale bars = 1 mm.

Figure S4

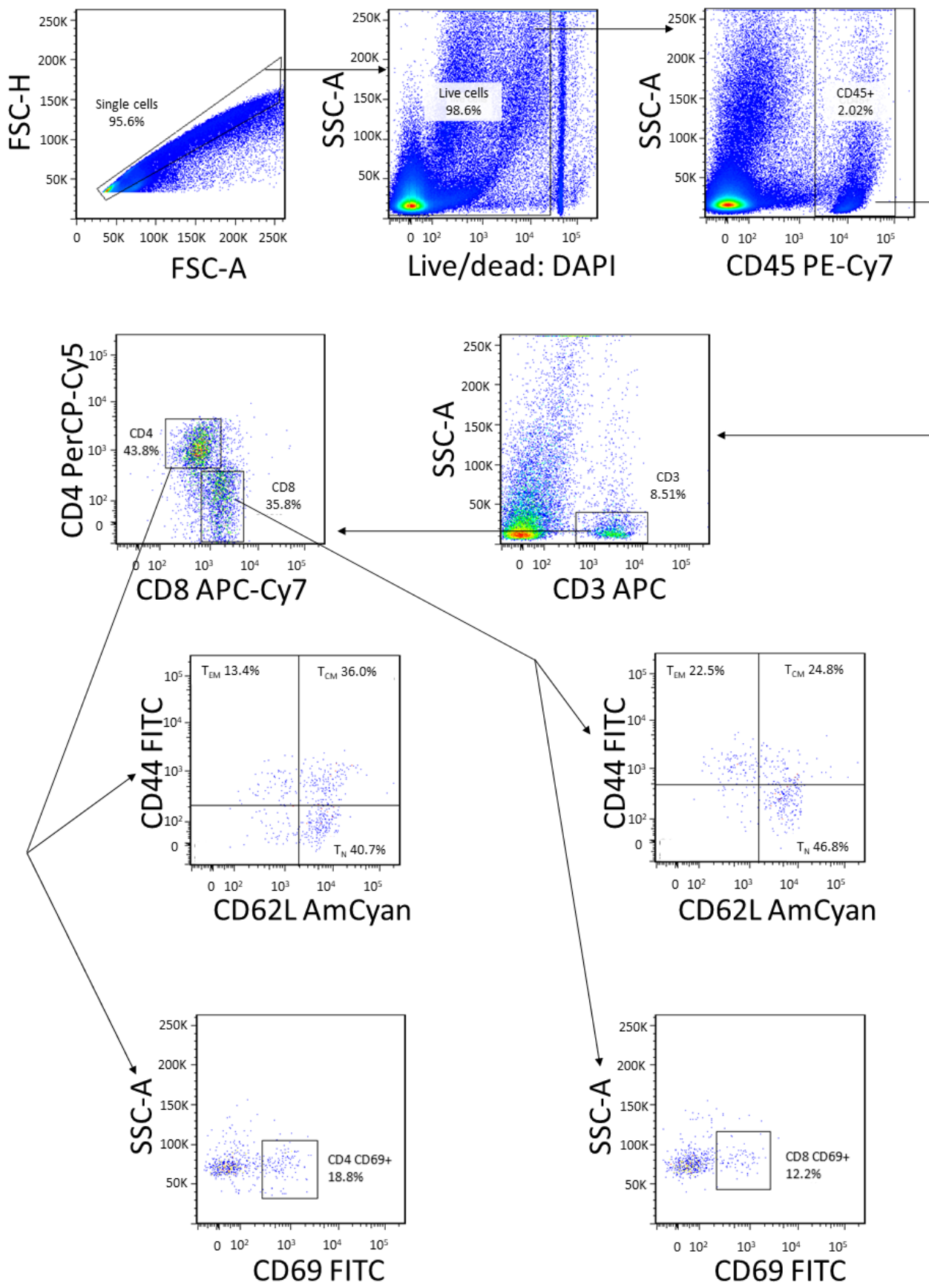


Figure S4: Gating strategy for the assessment of T-cell subsets: Dot-plots that display the gating strategy utilized for determination of T-cell subsets in the aortas (and spleens) of control, HS treated mice, with or without AngII infusion. The arrows show the hierarchy of the gating strategy. First, cells were selected on their FSC/SSC pattern and cell-doublets were eliminated. Dead cells were excluded from the analysis by DAPI-staining and subsequently leukocytes were identified as CD45⁺. Next, CD3⁺ T cells and their CD4⁺ and CD8⁺ subsets were identified. Finally, memory and early activated CD4⁺/CD8⁺ T cells were analyzed by expression of CD44/CD62L and CD69, respectively. Naïve T cells = CD44⁻/CD62L⁺, effector memory = CD44⁺/CD62L⁻, central memory CD44⁺/CD62L⁺. All thresholds and gates were set using fluorescence minus one (FMO) controls.

Figure S5

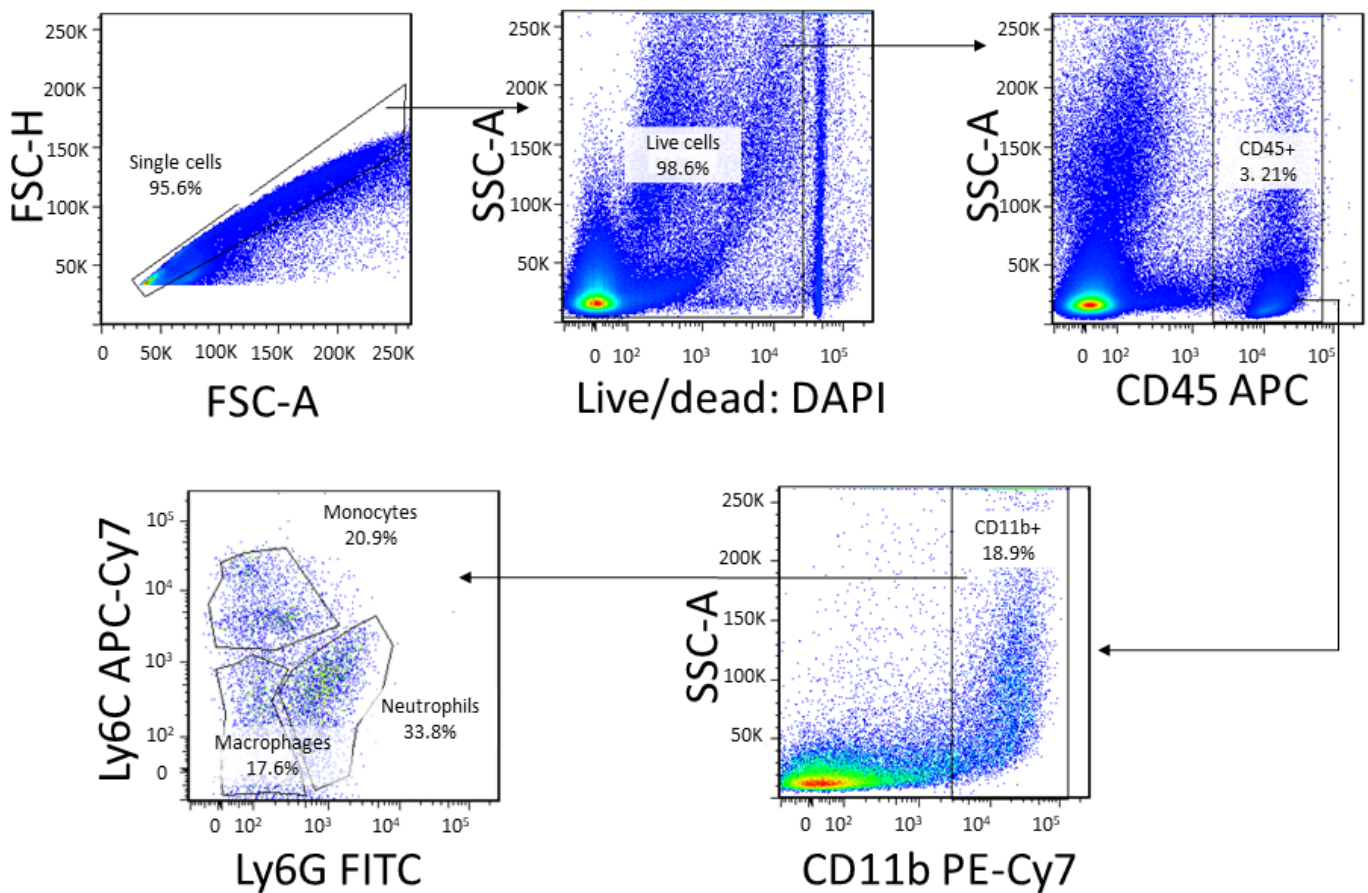


Figure S5: Gating strategy for the assessment of monocytes, macrophages, and neutrophils: Dot-plots were used to display the gating strategy utilized for determining the absolute counts and the relative amounts of aortic (or splenic) monocytes, macrophages, and neutrophils. CD45⁺/CD11b⁺ cells were identified and monocytes, macrophages and neutrophils were distinguished via the expression of Ly6G and Ly6C. Monocytes = Ly6c⁺, L6G⁻; Neutrophils = Ly6c⁻, L6G⁺; Macrophages = Ly6c⁻, L6G⁻.

Figure S6

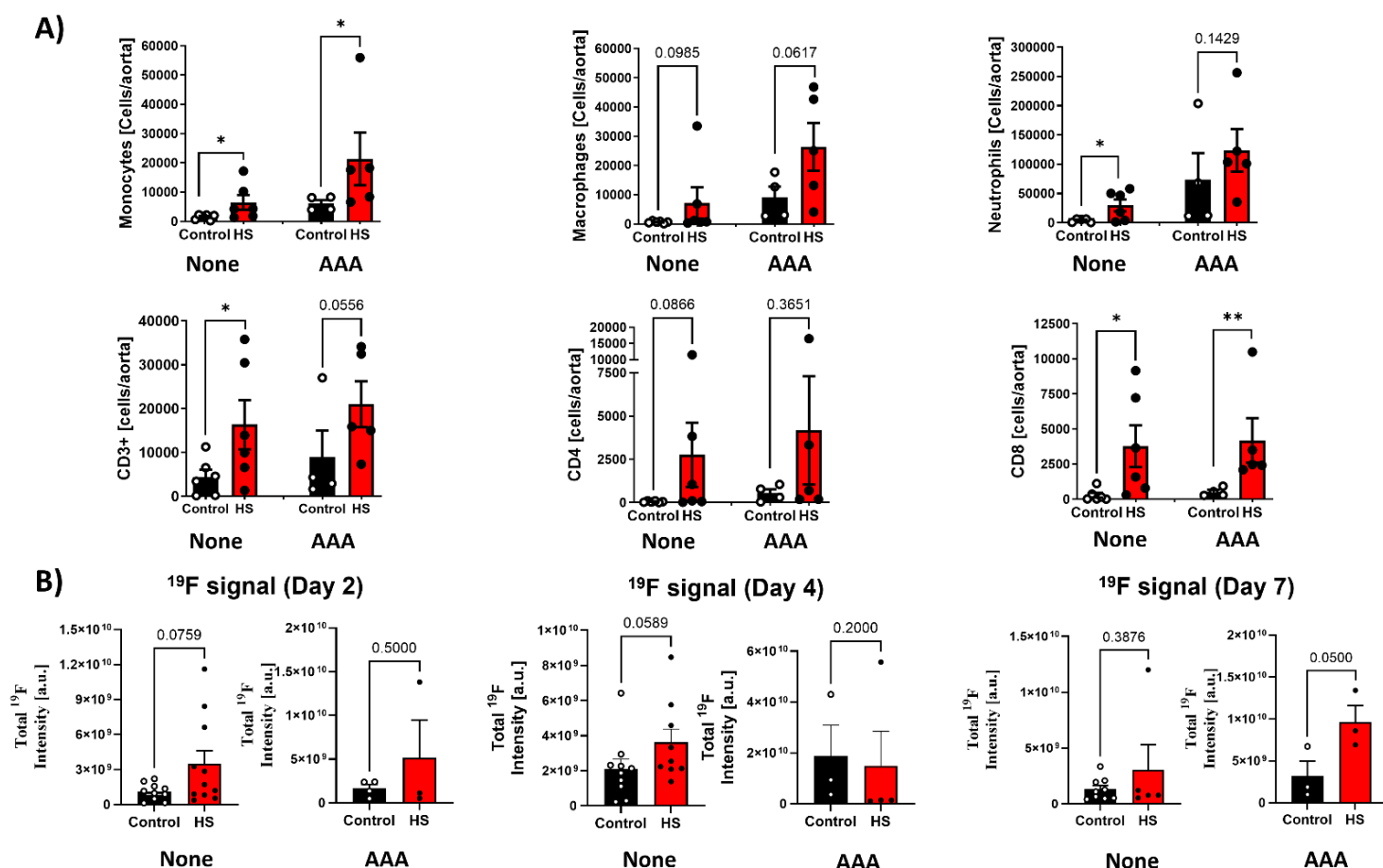


Figure S6: Effect of the incidence of AAA on immune cell distribution: A-F: Comparison of immune cell abundance in the aorta of mice that had AAA or not from both the control and transient high salt group at day 10 of AngII infusion. Control and HS from AAA or none-AAA. n=4-6, *p<0.05, **p<0.01, by unpaired, one-tailed t-test for normally distributed and one-tailed Mann-Whitney U test was used when normal distribution was not achieved. A: Monocytes. B: Macrophages. C: Neutrophils. D: CD3 T-cells. E: CD4 T-cells. F: CD8 T-cells. G-I: Quantification of the total ¹⁹F signal intensity in the aortic wall at different time points. G: day 2, H: day 4, I: day 7 of Ang II infusion. *p<0.05 two-tailed Mann-Whitney U test. AAA or none Control: n=5-11, AAA or none HS: n=3-4

Figure S7

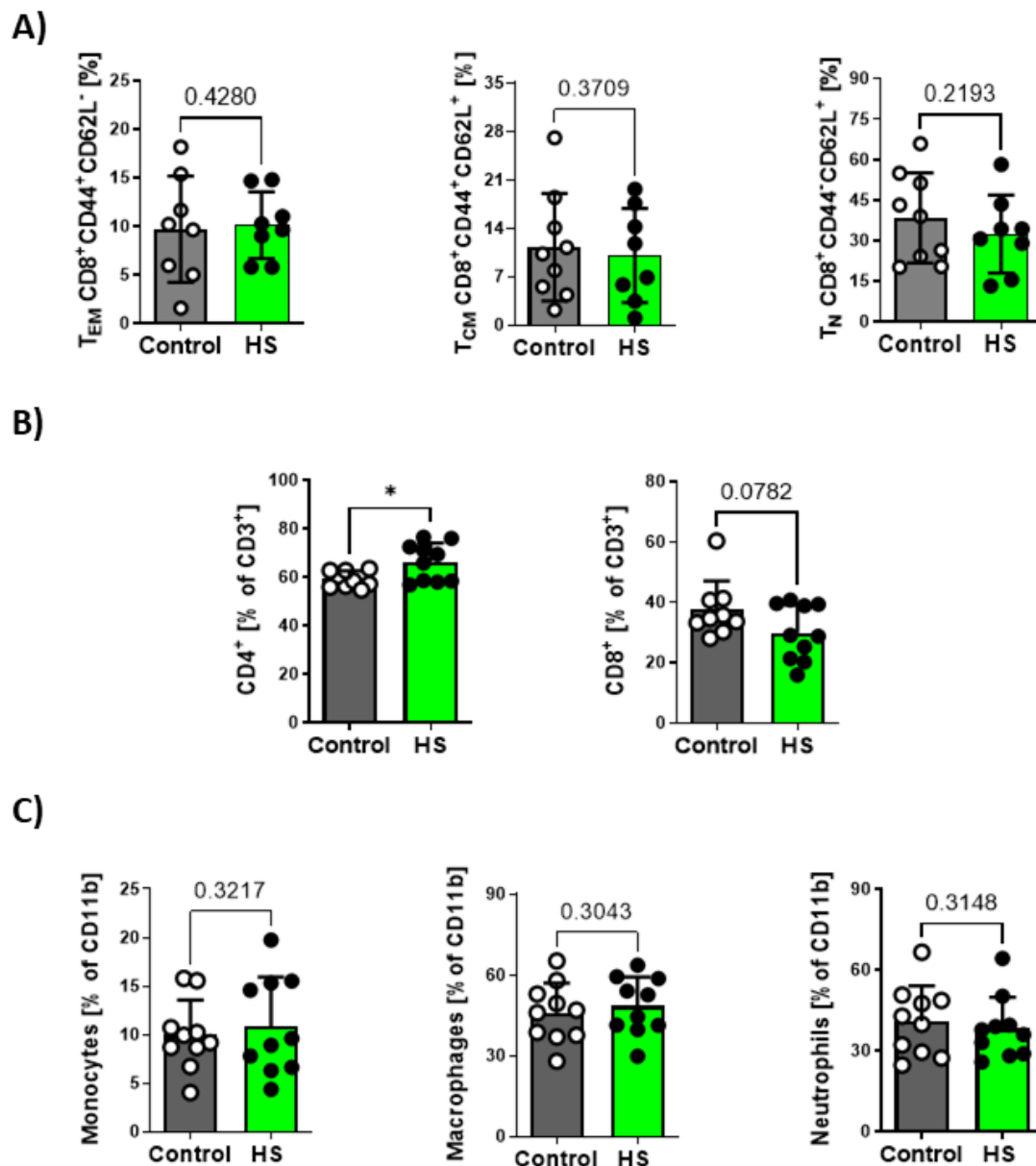


Figure S7: Aortic immune cells after transient HS: Flow cytometric analysis of T cell subtypes and myeloid immune cells in the aorta of mice subjected to high salt (HS) for two weeks followed by one week of normal tap water, but without AngII treatment. **A)** Flow cytometric analysis of memory $CD8^+$ T cells derived from the aortas of control animals and mice subjected to HS. Effector memory T cells (T_{EM}) = $CD44^+/CD62L^-$; Central memory T cells (T_{CM}) = $CD44^+/CD62L^+$, and Naïve T cells (T_N) = $CD44^+/CD62L^+$. Control n=8-9, HS n=8. Not significant by one-tailed t-test with/without Welch's correction. **B)** Control n=9, HS

n=10. Relative amount of CD4⁺ (left) or CD8⁺ (right) as a percentage of CD3⁺ T cells in the aorta. C) Flow cytometric analysis of macrophages, monocytes and neutrophils in the aorta of mice treated with or without transient high salt (HS). The graphs show the percentage of monocytes, macrophages, and neutrophils out of all CD11b⁺ cells. Control & HS n=10. Statistical analysis: One-tailed, unpaired t-test with/without Welch's correction.

Figure S8

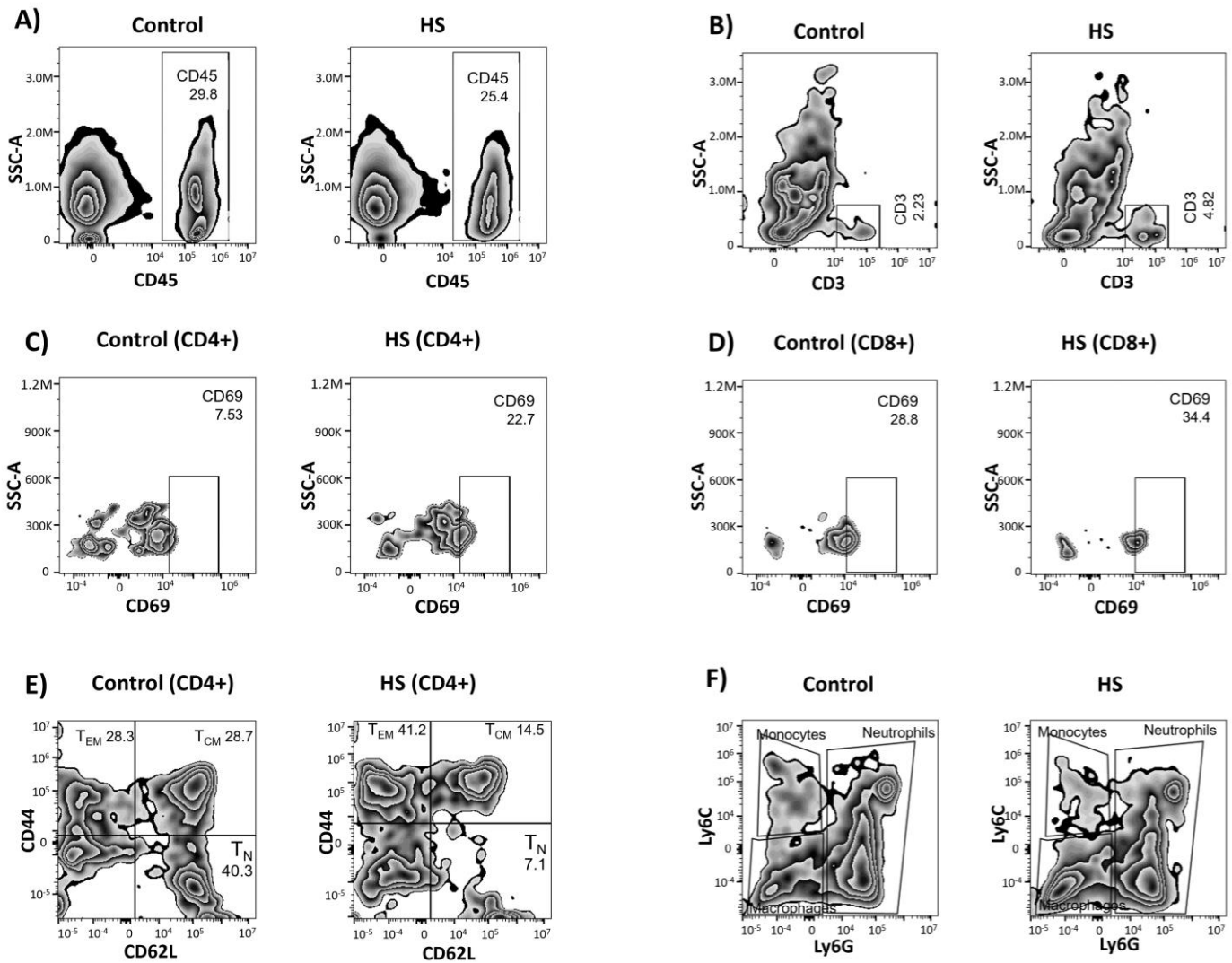


Figure S8: Flow cytometry of aortic immune cells after high salt but without AngII: ApoE^{-/-} mice were subjected to high salt (or tap water as control) for two weeks, followed by a washout period of one week. Aortas were excised, digested and analysed by flow cytometry. Displayed are zebra plots for the analysis of all aortic immune cell subsets. **A)** CD45 immune cells, **B)** CD3⁺ cells, **C)** CD4⁺CD69⁺, **D)** CD8⁺CD69⁺, **E)** Effector memory T cells (T_{EM}) = CD44⁺/CD62L⁻; Central memory T cells (T_{CM}) = CD44⁺/CD62L⁺, and Naïve T cells (T_N) = CD44⁻/CD62L⁺, **F)** Monocytes, macrophages, and neutrophils.

Figure S9

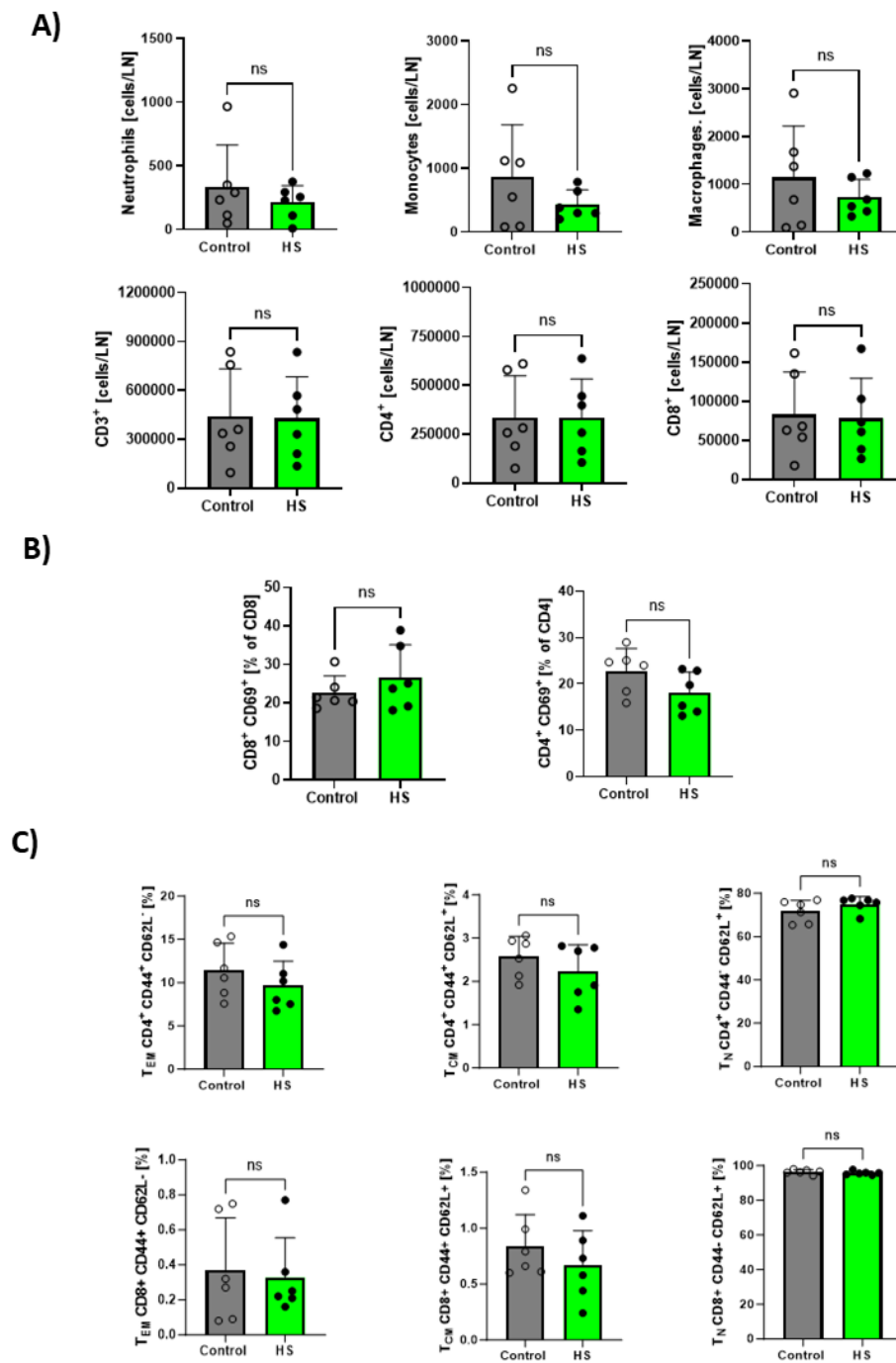


Figure S9: Flow cytometric analysis of immune cells in the mesenteric lymph nodes after HS treatment: ApoE^{-/-} mice received 1 % NaCl (or tap water as control) for 2 weeks (no AngII). Mesenteric lymph nodes were excised and immune cells were isolated and analyzed by flow cytometry. **(A)** Cell counts per mesenteric lymph node of neutrophils, monocytes, and macrophages, CD3⁺ and CD8⁺/CD4⁺ T cells. **(B)** CD69⁺ CD4⁺ and CD8⁺ T cells. **(C)**

CD4⁺/CD8⁺ effector memory T cells (TEM) = CD44⁺/CD62L⁻; Central memory T cells (TCM) = CD44⁺/CD62L⁺, and Naïve T cells (TN) = CD44⁻/CD62L⁺. Control n=6, HS n=6. Statistical analysis: One-tailed, unpaired t-test or Mann-Whitney U test. ns: not significant.

Figure S10

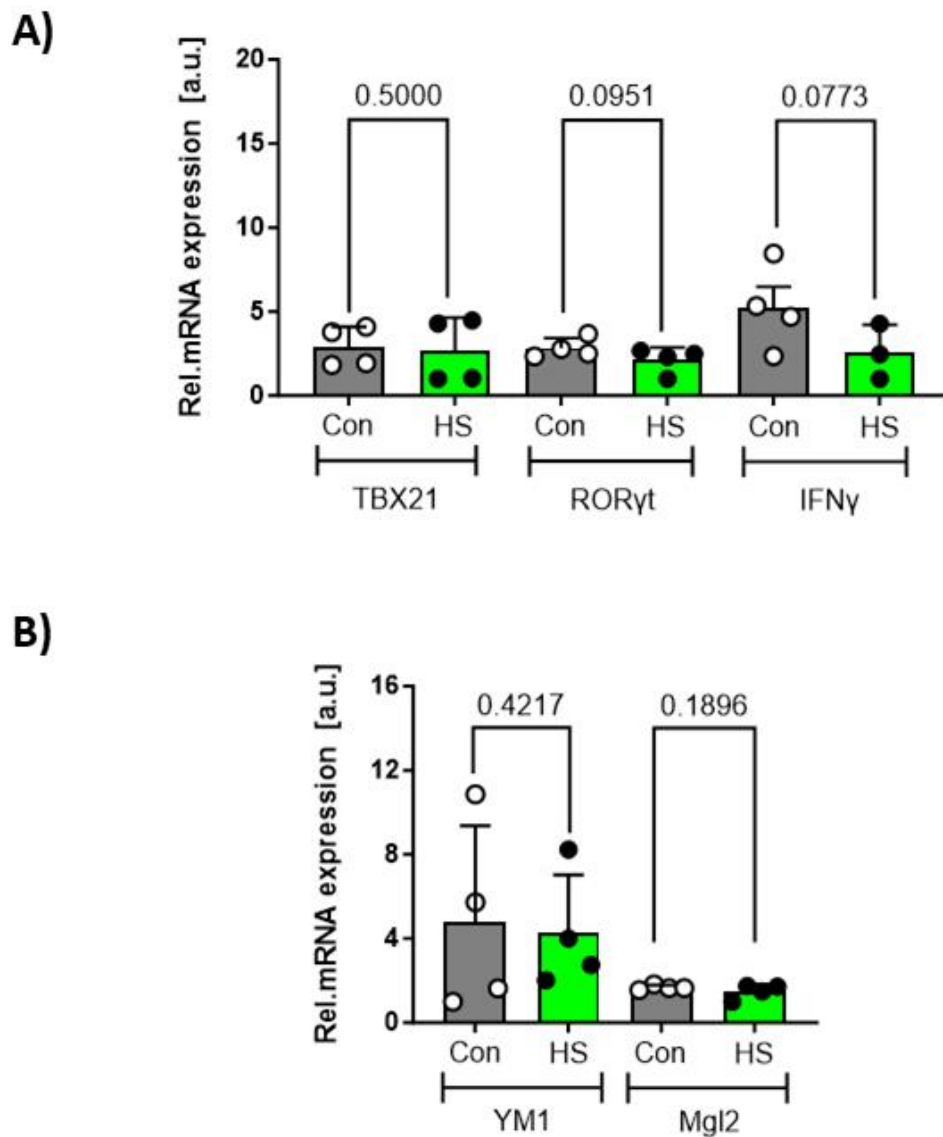


Figure 10: Markers of immune cell differentiation in the aorta after transient HS: A) Relative expression of mRNA-levels of T cell marker genes (*TBX21* and *IFN γ* = T_H1 cells; *ROR γ t* = T_H17 cells) or **B)** the M1/M2 macrophage markers (*YM1* and *Mgl2*) in aortas derived from control animals (grey) or mice subjected to transient high salt (HS; green) before AngII infusion. Control n=4, HS n=4. Data were analyzed by one-tailed t-test with Welch's correction or Mann-Whitney U test (*TBX21*).

Figure S11

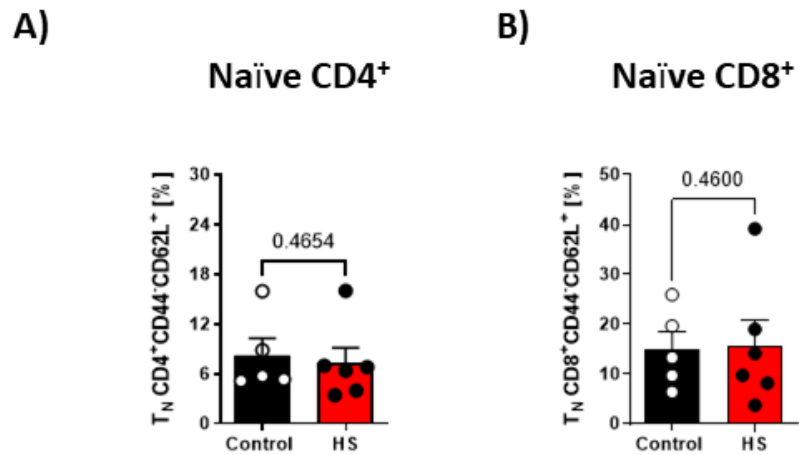


Figure S11: A) Flow cytometric analysis of naïve CD4⁺ T cells (T_N) = CD44⁺/CD62L⁺ Control n=5, HS n=6. Not significant by unpaired, one-tailed Mann-Whitney U test. **B)** Flow cytometric analysis of naïve CD8⁺ T-cells (T_N) = CD44⁺/CD62L⁺ Control n=5, HS n=6. Not significant by unpaired, one-tailed t-test with Welch's correction.

Figure S12

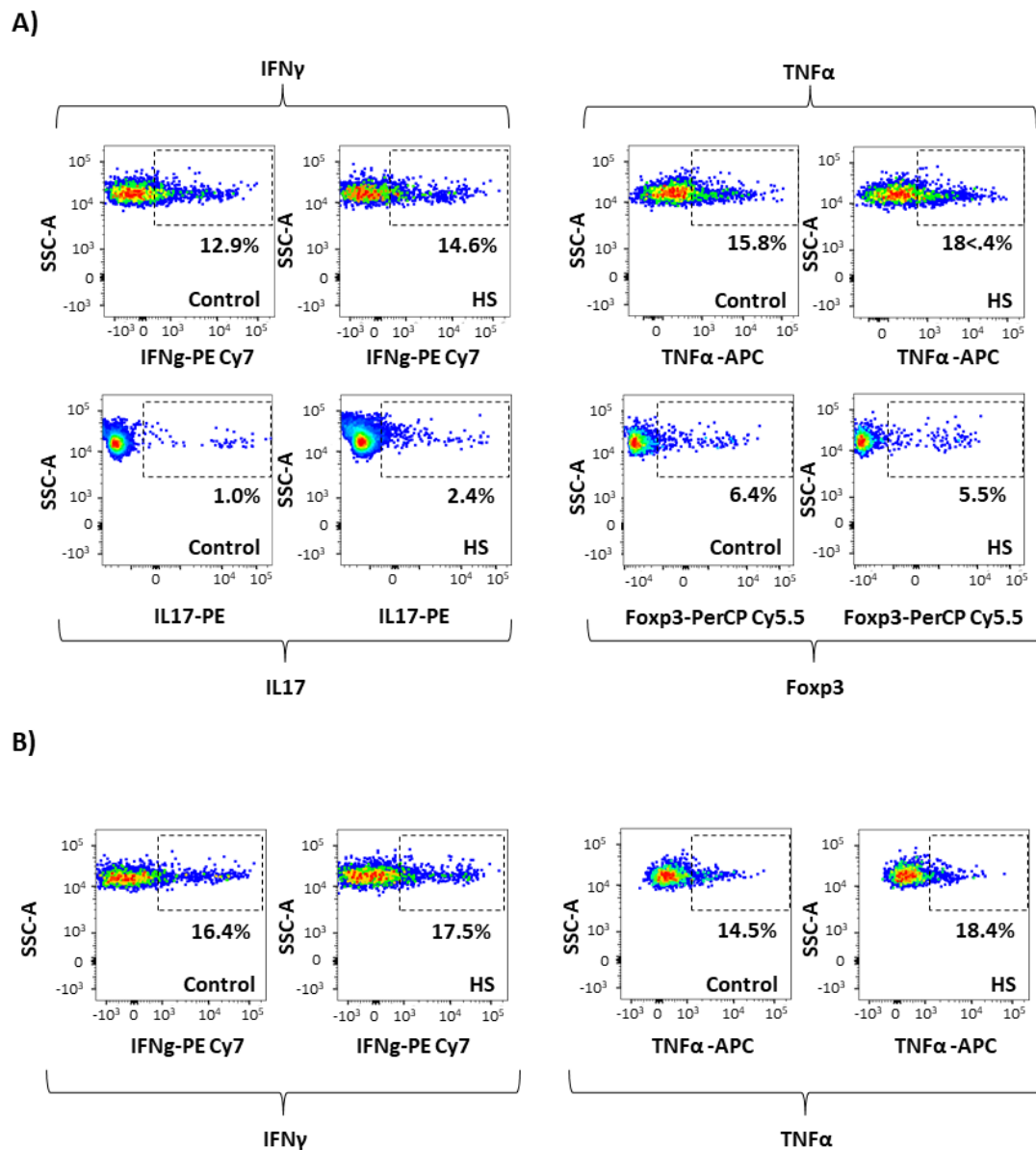
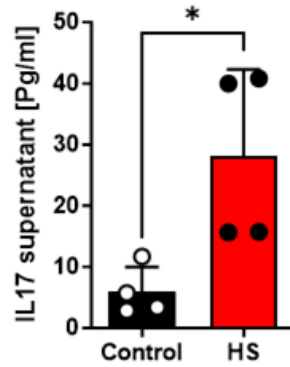


Figure S12: Flow cytometry of intracellular markers in splenic CD4⁺ and CD8⁺ T cells:

A) Upper panel: Pseudocolor dot-plots showing the intracellular expression of IFN γ , TNF α , IL17 and Foxp3 in aortic CD4⁺ T cells of control mice (Control) and mice treated transiently with high salt (HS) followed by a one week washout period with normal tap water. Control and HS were subsequently treated with AngII for an additional ten days. **B)** Intracellular expression of TNF α or IFN γ in CD8⁺ T cells derived from aortas of control and HS mice. The numbers indicate the relative amount of the cells that express the respective marker.

Figure S13

A)



B)

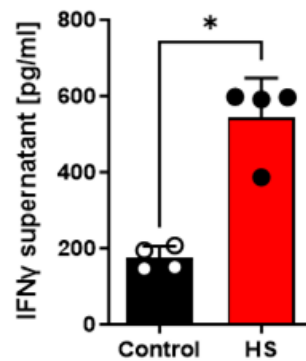


Figure S13: High salt enhances IL17 and IFN γ secretion in CD4⁺/CD8⁺ T cells: A/B)

Isolated splenic CD4⁺ or CD8⁺ T cells were aCD3/aCD28 stimulated in the presence or absence of additional 40 mM NaCl in the medium. After 72h, the supernatant was removed and IL17/IFN γ concentrations were analyzed in the supernatant by enzyme-linked immunosorbent assay. Data are mean values of n=4 individual experiments. *p<0.05, unpaired, one-tailed Mann-Whitney U test.

Figure S14

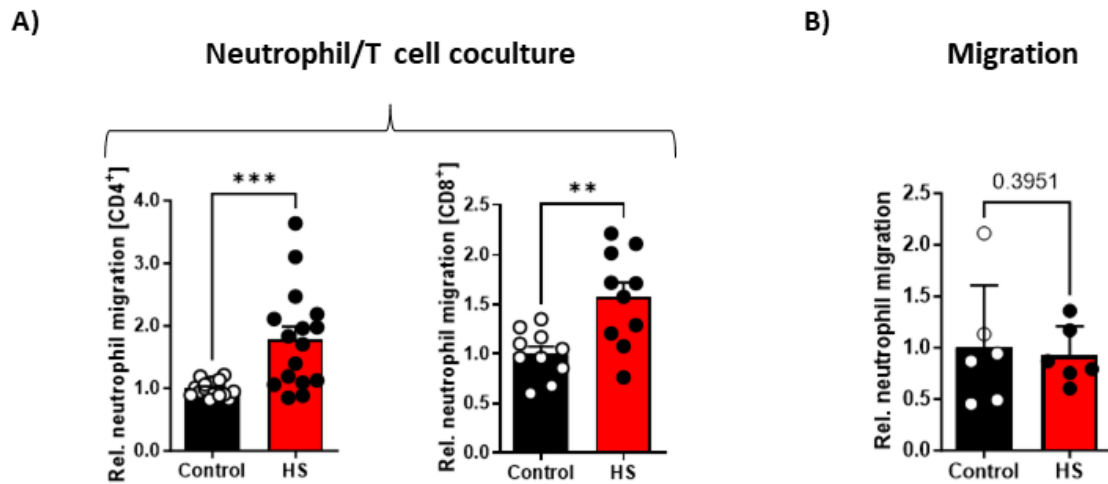
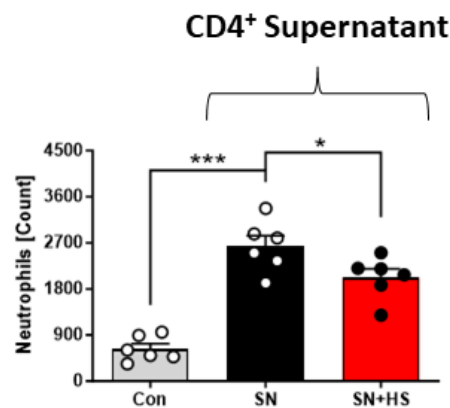


Figure S14: Impact of high salt on neutrophils migration *in vitro*: **A)** Migration of neutrophils (Boyden chamber assay towards fMLP) after coculture with CD4⁺ or CD8⁺ cells that have been CD3/CD28 activated under normal or HS conditions. Control and HS of n=10-16, **p<0.01, ***p<0.001, by unpaired, one-tailed t-test with Welch's correction. **B)** Migration of neutrophils towards fMLP after culture under normal or HS conditions. Data was normalized to the mean values of the control group. Control and HS n=6, not significant by one-tailed, unpaired t-test with Welch's correction.

Figure S15

A)



B)

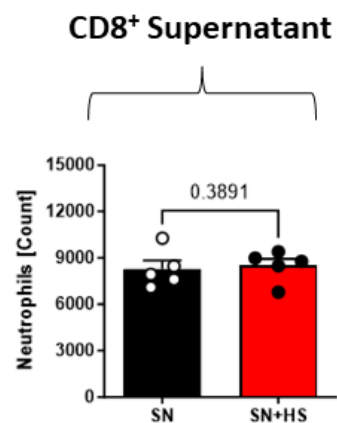


Figure S15: Neutrophil migration after stimulation with supernatant from activated CD4⁺ or CD8⁺ T-cells: A/B) Isolated splenic CD4⁺ or CD8⁺ T cells were CD3/CD28 stimulated in the presence or absence of additional 40 mM NaCl in the medium. After 72h, the supernatant was removed and added to neutrophils isolated from the bone marrow. Migration was analyzed in a Boyden chamber assay with fMLP as a chemoattractant. Con = neutrophils without T cell supernatant, SN = neutrophils + supernatant of CD4⁺ (A) or CD8⁺ cells under normal salt conditions. SN + HS: supernatant of CD4⁺/CD8⁺ T cells stimulated and cultivated with high salt. A) Con: n=6, SN & SN+HS: n=6; for CD4⁺ supernatant. **p<0.01, ***p<0.001,

unpaired, one-tailed t-test with Welch's correction. B) SN and SN+HS: $n=5$. Not significant by unpaired, one-tailed t-test.

Figure S16

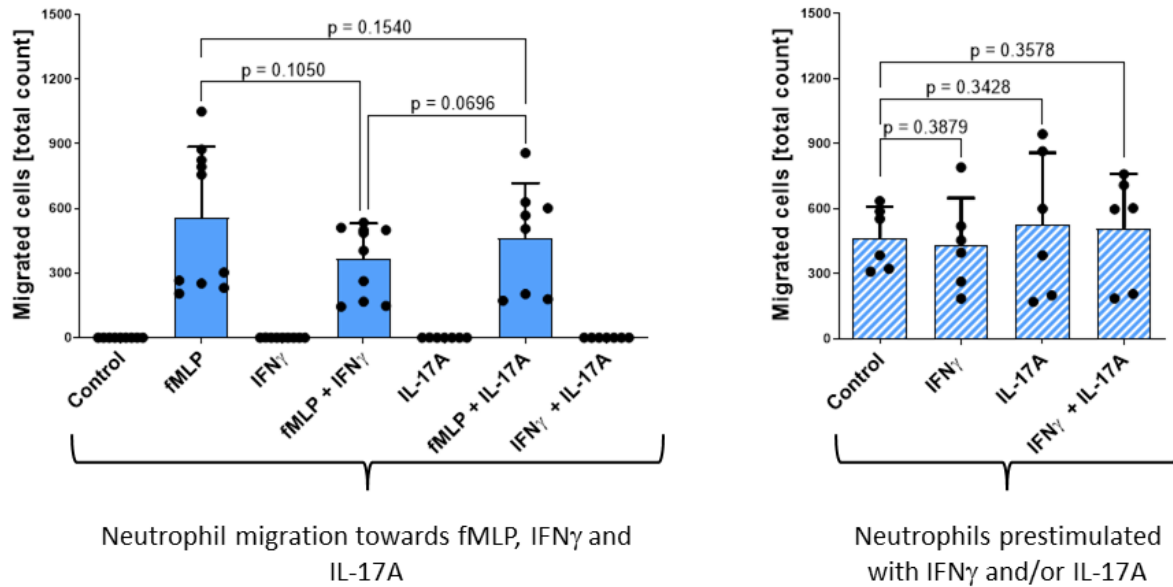


Figure S16: Impact of IFN γ and IL17 on neutrophil migration: Bone marrow neutrophils were isolated from C57BL/6 mice and subjected to a boyden chamber migration assay. **Left:** fMLP, IFN γ , IL17A or combinations of these molecules were added to the lower chamber and the amount of migrated neutrophils was determined after 2h by flow cytometry. As a control, no chemokine/cytokine was added to the lower chamber. **Right:** neutrophils were preincubated with IFN γ , IL17A or IFN γ + IL17A and afterwards the migration towards fMLP was analyzed. Data are mean values \pm SD of n=6-8. Unpaired t-test or two-tailed Mann-Whitney U test.

Figure S17

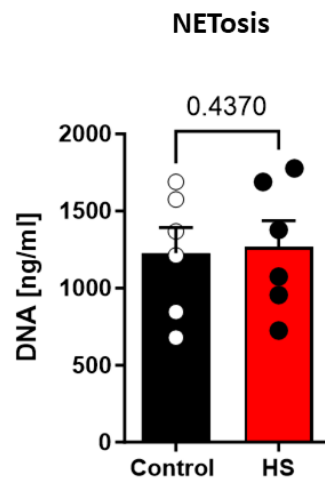


Figure S17: NETosis of neutrophil granulocytes: Bone marrow derived murine neutrophils from C57BL/6 mice were cocultured with anti-CD3/CD28 activated CD4⁺ T cells and further cultivated under HS or with normal salt concentrations. DNA release was determined in the supernatant of the cells using PicoGreen and subsequent analysis in a fluorescence microplate reader. Control and HS n=6, not significant, by one-tailed, unpaired t-test.